



รายงานวิจัยฉบับสมบูรณ์

โครงการ<u>การปรับปรุงคุณภาพของภาพวิดิโอโดยใช้วิธีการสร้างคืนภาพความละเอียด</u>
<u>สูงยิ่งแบบการประมาณแบบ Robust Stochastic ด้วยแบบจำลองการบันทึกภาพที่ถูก</u>
<u>ปรับปรุงใหม่ (Video Enhancement Using An Iterative SRR Based On A Robust Stochastic Estimation With An Improved Observation Model)</u>

โดย <u>ผศ.ดร. วรพจน์ พัฒนวิจิตร</u>

รูปแบบ Abstract (บทคัดย่อ) (ภาษาไทยและภาษาอังกฤษ)

Project Code: MRG5180263

Project Title: การปรับปรุงคุณภาพของภาพวิดิโอโดยใช้วิธีการสร้างคืนภาพความละเอียดสูงยิ่งแบบ การประมาณแบบ Robust Stochastic ด้วยแบบจำลองการบันทึกภาพที่ถูกปรับปรุงใหม่ (Video Enhancement Using An Iterative SRR Based On A Robust Stochastic Estimation With An Improved Observation Model)

Investigator:

ผศ.ดร. วรพจน์ พัฒนวิจิตร มหาวิทยาลัยอัสสัมชัญ

รศ.ดร. สมชาย จิตะพันธ์กุล จุฬาลงกรณ์มหาวิทยาลัย

E-mail Address:

Patanavijit@yahoo.com

Project Period:

3 Years

Abstract: This paper proposes two novel algorithms: the improved observation model and the several robust norms for SRR algorithm. The proposed observation model assumes the affine motion as the relationship between blocked images (the current frame and the reference: frame). It is applicable to not only the standard sequences but also real sequences with complex motion hence it can be implemented in the previous SRR algorithms. Moreover, it can be implemented in motion estimation algorithm. To realize the implementation of the proposed sub-pixel image registration, the fast algorithm is designed to reduce the computational load for the proposed sub-pixel registration. Due to its high performance and low complexity, this paper considers the use of a regularized maximum likelihood estimator in the image estimation process. The real noise models that corrupt the measure sequence are unknown therefore SRR algorithm using L1 or L2 norm may degrade the image sequence rather than enhance it. The novel robust (Hampel, Andrew's Sine, Geman&McClure and Leclerc) are proposed into the model of the SRR framework using the proposed registration. The experimental results demonstrate the effectiveness of proposed methods and its superiority to other SRR algorithms based on L1 and L2 norm with classical observation model for several noise models (such as Noiseless, AWGN, Poisson Noise, Salt&Pepper Noise and Speckle Noise) at different noise power.

Keywords: Digital Image Processing, Digital Video Processing, Image Reconstruction

TECHNICAL REPORT

VIDEO ENHANCEMENT USING AN ITERATIVE SRR BASED ON A ROBUST STOCHASTIC ESTIMATION WITH AN IMPROVED OBSERVATION MODEL[†]

Vorapoj Patanavijit, B.Eng., M.Eng., Ph.D.

Department of Computer and Network Engineering, Faculty of Engineering, Assumption University, Bangkok, 10240 Thailand, Tel: +66 (0)2 3004543-62 Ext 3725, 3736, Mob: +66 (0)81 255-2706 Fax: +66 (0)2 719-1503, Email: Patanavijit@yahoo.com

ABSTRACT This paper proposes two novel algorithms: the improved observation model and the several robust norms for SRR algorithm. The proposed observation model assumes the affine motion as the relationship between blocked images (the current frame and the reference frame). It is applicable to not only the standard sequences but also real sequences with complex motion hence it can be implemented in the previous SRR algorithms. Moreover, it can be implemented in motion estimation algorithm. To realize the implementation of the proposed sub-pixel image registration, the fast algorithm is designed to reduce the computational load for the proposed sub-pixel registration. Due to its high performance and low complexity, this paper considers the use of a regularized maximum likelihood estimator in the image estimation process. The real noise models that corrupt the measure sequence are unknown therefore SRR algorithm using L1 or L2 norm may degrade the image sequence rather than enhance it. The novel robust (Hampel, Andrew's Sine, Geman&McClure and Leclerc) are proposed into the model of the SRR framework using the proposed registration. The experimental results demonstrate the effectiveness of proposed methods and its superiority to other SRR algorithms based on L1 and L2 norm with classical observation model for several noise models (such as Noiseless, AWGN, Poisson Noise, Salt&Pepper Noise and Speckle Noise) at different noise power.

Research Field: Digital Image Processing, Digital Video Processing, Image Reconstruction

[†]This technical report is a partial fulfillment of the requirement for "VIDEO ENHANCEMENT USING AN ITERATIVE SRR BASED ON A ROBUST STOCHASTIC ESTIMATION WITH AN IMPROVED OBSERVATION MODEL" that has been supported by Research Grant for New Scholar (MRG5180263) from TRF (Thai Research Fund) and CHE (Commission on Higher Education) under Assumption University (Thailand).

1. INTRODUCTION

1.1 INTRODUCTION

Several distorting processes affect the quality of image sequences or video acquired by commercial digital cameras. Some of the more important distorting effects include warping, blurring, down sampling and additive noise. The term SRR (Super-Resolution Reconstruction) ranges from blur removal by Interframe in single image to the creation of a single high resolution image from multiple low resolution images having relative sub-pixel displacements. In all cases, the goal of SRR is to remove the effect of possible blurring and noise in the LR images and to obtain images with resolutions that go beyond the conventional limits of the uncompensated imaging system. Thus, the major advantage of this approach is that the cost of implementation is reduced and the existing low resolution (LR) imaging systems can still be utilized. Therefore, applications for the SRR techniques from image sequences grow rapidly as the theory gains exposure. Continuing researches and the availability of fast computational machineries have made these methods increasingly attractive in applications requiring the highest restoration performance. SRR techniques have already been applied to problems in a number of applications such as satellite imaging, astronomical imaging, video enhancement and restoration, video standards conversion, confocal microscopy, digital mosaicing, aperture displacement cameras, medical imaging, diffraction tomography and video freeze frame.

The spatial resolution that represents the number of pixels per unit area in an image is the principal factor in determining the quality of an image. With the development of image processing applications, there is a great demand for high-resolution (HR) images since HR images offer not only the viewer a pleasing picture but also additional details that are important for the analysis in many applications. The most direct solution to increase spatial resolution is to reduce the pixel size (i.e., increase the number of pixels per unit area) by sensor manufacturing techniques. As the pixel size decreases, however, the amount of light available also decreases. It generates shot noise that severely degrades the image quality. To reduce the pixel size without suffering the effects of shot noise, therefore, there exists the limitation of the pixel size reduction, and the optimally limited pixel size is estimated at about 40 μm² for a 0.35 μm CMOS processor [57, 95]. The current image sensor technology has almost reached this level. Another approach for enhancing the spatial resolution is to increase the chip size, which leads to an increase in capacitance. Since large capacitance makes it difficult to speed up a charge transfer rate, this approach is not considered effective. The high cost for high precision optics and image sensors is also an important concern in many commercial applications regarding HR imaging therefore many digital image restoration techniques have been proposed since 1970s.

Image restoration techniques are broadly categorized into two classes based on the number of observed frames. Specifically, the categorization is into the classes of single-frame and multi-frame restoration methods. The classical image restoration problem is concerned with restoration of a single output image from a single degraded observed image and the literature on the restoration of a single input frame is extensive and spans several decades [15, 16, 17, 33, 64, 80, 83]. While the field of single frame image restoration appears to have matured, digital video has raised many new restoration problems for image processing researchers [125]. Since video typically consists of a sequence of similar, though not identical frames, it becomes possible to utilize the inter-frame motion information in processing the video data. This led to the development of image sequence processing techniques such as motion estimation [11, 39, 45, 94, 106, 108, 124, 125], image sequence interpolation [80],

image registration [3, 6, 18] and standards conversion [125]. Image restoration researchers also recognized the potential of image restoration in increasing spatial resolution using the information totally contained in an image sequence as compared with that available from a single image. This led naturally to algorithms which apply motion compensation and image restoration techniques to produce high-quality and high-resolution still images from image sequences called Super-Resolution Reconstruction (SRR).

In the last two decades, the enlargement in the extensive use of digital imaging technologies in consumer (e.g., digital video) and other markets (e.g., security and military) has brought with it a simultaneous demand for higher-resolution (HR) images. The demand for such images can be partially met by algorithmic advances in SRR technology in addition to hardware development. Such HR images not only give the viewer a more pleasing picture but also offer additional details that are important for subsequent analysis in many applications. SRR algorithms [9, 20, 57, 63, 95] investigate the relative motion information between multiple low-resolution (LR) images or a video sequence and increase the spatial resolution by fusing them into a single frame. In doing so, it also removes the effect of possible blurring and noise in the LR images. In summary, the SRR algorithm estimates an HR image with finer spectral details from multiple LR observations degraded by blur, noise, and aliasing.

The major advantage of this approach is that the cost of implementation is reduced and the existing LR imaging systems can still be utilized. Thus, applications for the techniques of SRR from image sequences grow rapidly as the theory gains exposure. Continuing researches and the availability of fast computational machineries have made these methods increasingly attractive in applications requiring the highest restoration performance. SRR techniques have already been applied to problems in a number of applications such as satellite imaging, astronomical imaging, video enhancement and restoration, video standards conversion, confocal microscopy, digital mosaicing, aperture displacement cameras, medical computed tomographic imaging, diffraction tomography, video freeze frame and hard copy.

In SRR, typically, the LR images represent different "looks" at the same scene [95]. That is, LR images are subsampled (aliased) as well as shifted with sub-pixel precision. If the LR images are shifted by integer units, then each image contains the same information, and thus there is no new information that can be used to reconstruct a HR image. If the LR images have different sub-pixel shifts from each other and if aliasing is present, however, then each image cannot be obtained from the others. In this case, the new information contained in each LR image can be exploited to obtain a HR image. To obtain different looks at the same scene, some relative scene motions must exist from frame to frame via multiple scenes or video sequences. Multiple scenes can be obtained from one camera with several captures or from multiple cameras located in different positions. These scene motions can occur due to the controlled motions in imaging systems, e.g., images acquired from orbiting satellites. The same is true of uncontrolled motions, e.g., movement of local objects or vibrating imaging systems. If these scene motions are known or can be estimated within sub-pixel accuracy and if we combine these LR images then SRR is possible.

Most of the SRR registration techniques [95] are based on the sub-pixel translation motion assumption. This implies the observed images or sequences can be modeled by global or local uniform translation thus the traditional sub-pixel registration can not be applied on the real complex motion sequences and super-resolution applications can be applied only on the sequences that have simple translation motion. In addition to image registration, the robust estimation and high accurate image estimation is also required. The traditional estimated techniques for SRR, proposed in the past literatures [9, 20, 57, 63, 94, 95] are based on the simple estimation techniques such as L1 Norm or L2 Norm

Minimization. From these points of view, the SRR estimation technique and SRR sub-pixel registration for the real complex sequences is a very challenging topic because the performance of the registration and estimation techniques have a major impact on the performance of the SRR system.

In this section, the fundamental knowledge of the SRR algorithm is described. This includes a block diagram of observation model and SRR algorithm. The first step to comprehensively review the SRR problem is to formulate an observation model that relates the original HR image to the observed LR images. Several observation models have been explored in [95], and they can be broadly divided into the models for still images and for video sequence. To present a basic concept of SR reconstruction techniques, we employ the observation model for still images in [95] as shown in Figure 1.1, since it is rather straightforward to extend the still image model to the video sequence model.

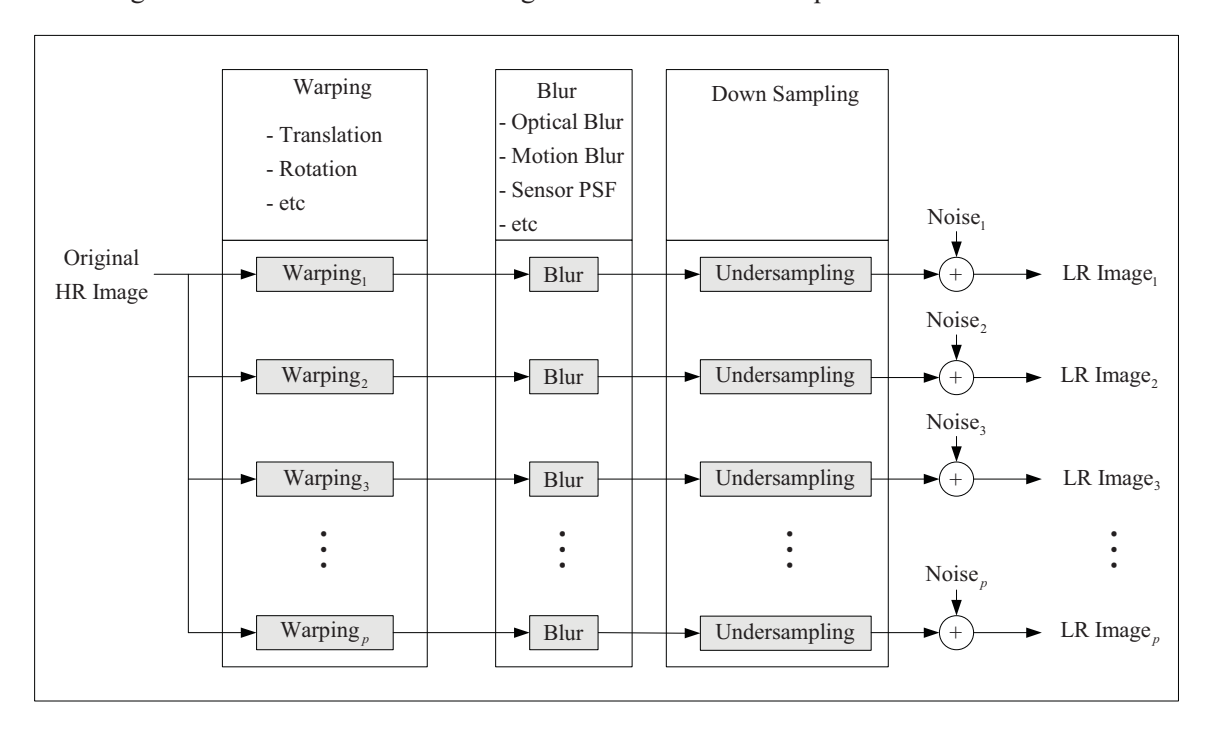


Figure 1.1: Block Diagram of Observation Model.

The motion that occurs during the image acquisition is represented by warping processes. It may contain global or local translation, rotation, and so on. Since this information is generally unknown, we need to estimate the scene motion for each frame with reference to one particular frame. The warping process performed on HR image is actually defined in terms of LR pixel spacing when we estimate it. Thus, this step requires interpolation when the fractional unit of motion is not equal to the HR sensor grid.

Blur may be caused by an optical system (e.g., out of focus, diffraction limit, aberration, etc.), relative motion between the imaging system and the original scene, and the point spread function (PSF) of the LR sensor. It can be modeled as linear space invariant (LSI) or linear space variant (LSV). In single image restoration applications, the optical or motion blur is usually considered. In the SRR, however, the finiteness of a physical dimension in LR sensors is an important factor of blur.. In the use of SRR algorithms, the characteristics of the blur are assumed to be known. However, if it is difficult to obtain this information, blur identification should be incorporated into the reconstruction procedure.

The downsampling process generates aliased LR images from the warped and blurred HR image. Although the size of LR images is the same here, in more general cases, we can address the different size of LR images by using a different downsampling matrix. Although the blur acts more or less as an anti-aliasing filter, in SR image reconstruction, it is assumed that aliasing is always present in LR images.

Most of the explored SRR algorithms [95] consist of the three stages illustrated in Figure 1.2: registration, interpolation and restoration (i.e., inverse procedure). These steps can be implemented separately or simultaneously according to the reconstruction methods adopted. The estimation methods of motion information [11, 12, 39, 40, 45, 74-78, 106, 108, 122] are referred to as registration methods [3, 6, 18], and it is extensively studied in various fields of image processing. In the registration stage, the relative shifts between LR images compared to the reference LR image are estimated with fractional pixel accuracy. Obviously, accurate sub-pixel motion estimation is a very important factor in the success of the SRR algorithm. Since the shifts between LR images are arbitrary, the registered HR image will not always match up to a uniformly spaced HR grid. Thus, nonuniform interpolation is necessary to obtain a uniformly spaced HR image from a composite of nonuniformly spaced LR images. Finally, image restoration is applied to the upsampled image to remove blurring and noise.

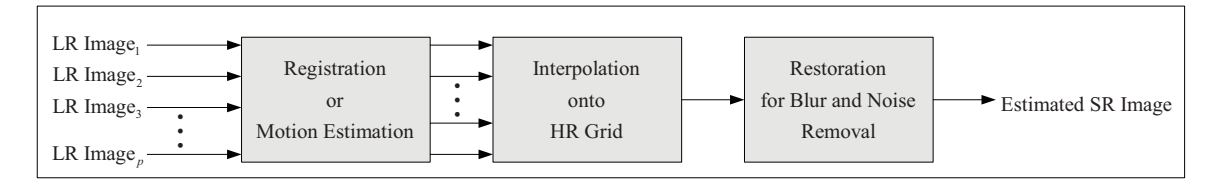


Figure 1.2: Super-Resolution Reconstruction (SRR) Block Diagram.

1.2 LITERATURE REVIEW

In this section, the relevant research papers, published in the conferences and journals are comprehensively reviewed. The Super-Resolution Reconstruction (SRR) idea was first presented by T. S. Huang and R. Y. Tsan [107] in 1984. They used the frequency domain approach to demonstrate the ability to reconstruct one improved resolution image from several downsampled noise-free versions of it, based on the spatial aliasing effect. Next, a frequency domain recursive algorithm for the restoration of super-resolution images from noisy and blurred measurements is proposed by S. P. Kim, N. K. Bose, and H. M. Valenzuela [102] in 1990. The algorithm using a weighted recursive least squares algorithm, is based on sequential estimation theory in the frequency-wavenumber domain, to achieve simultaneous improvement in signal-to-noise ratio and resolution from available registered sequence of low-resolution noisy frames. In 1993, S. P. Kim and Wen-Yu Su [103] also incorporated explicitly the deblurring computation into the high-resolution image reconstruction process because separate deblurring of input frames would introduce the undesirable phase and high wavenumber distortions in the DFT of those frames. Subsequently, M. K. Ng and N. K. Bose [62] proposed the analysis of the displacement errors on the convergence rate to the iterative approach for solving the transform based preconditioned system of equation in 2002 hence it is established that the used of the MAP, L2 Norm or H1 Norm regularization functional leads to a proof of linear convergence of the conjugate gradient method in terms of the displacement errors caused by the imperfect subpixel locations. Later, N. K. Bose, M. K. Ng and A. C. Yau [69] proposed the fast SRR algorithm, using MAP with MRF for blurred observation in 2006. This algorithm uses the reconditioned conjugated gradient method and FFT. Although the frequency domain methods are intuitively simple and computationally cheap, the observation model is restricted to only global translational motion and LSI blur. Due to the lack of data correlation in the frequency domain, it is also difficult to apply the spatial domain a priori knowledge for regularization.

The POCS formulation of the SRR was first suggested by Stark and Oskoui [95] in 1987. Their method was extended by Tekalp [95] to include observation noise in 1992. Although POCS is simple and can utilize a convenient inclusion of a priori information, this method has the disadvantages of nonuniqueness of solution, slow convergence and a high computational cost. Next, A. J. Patti and Y. Altunbasak proposed [2] a SRR (Super-Resolution Reconstruction) using ML estimator with POCS-based regularization in 2001 and Y. Altunbasak, A. J. Patti, and R. M. Mersereau [126] proposed a Super-Resolution Reconstruction (SRR) for the MPEG sequences in 2002. They proposed a motion-compensated, transform-domain super-resolution procedure that directly incorporates the transform-domain quantization information by working with the compressed bit stream. Later, B. K. Gunturk and Y. Altunbasak and R. M. Mersereau [7] proposed a ML super-resolution with regularization based on compression quantization, additive noise and image prior information in 2004. Next, H. Hasegawa, T. Ono, I. Yamada and K. Sakaniwa proposed iterative SSR using the Adaptive Projected Subgradient method for MPEG sequences in 2005 [27].

The MRF or Markov/Gibbs Random Fields [35-38, 43-44, 90-91] are proposed and developed for modeling image texture during 1990-1994. Due to MRF (Markov Random Field) that can model the image characteristic especially on image texture, C. Bouman and K. Sauer [10] proposed the single image restoration algorithm using MAP estimator with the GGMRF (Generalized Gaussian-Markov Random Field) prior in 1993. Later, R. L. Stevenson, B. E. Schmitz and E. J. Delp [82] proposed the single image restoration algorithm using ML estimator with the Discontinuity Persevering Regularization in 1994. R. R. Schultz and R. L. Stevenson [88] proposed the single image restoration algorithm using MAP estimator with the HMRF (Huber-Markov Random Field) prior in 1994. Next, the Super-

Resolution Reconstruction algorithm using MAP estimator (or the Regularized ML estimator), with the HMRF prior was proposed by R. R. Schultz and R. L. Stevenson [89] in 1996. The blur of the measured images is assumed to be simple averaging and the measurements additive noise is assumed to be independent and identically distributed (i.i.d.) Gaussian vector. In 2006, R. Pan and S. J. Reeves [87] proposed single image MAP estimator restoration algorithm with the efficient HMRF prior using decomposition-enabled edge-preserving image restoration in order to reduce the computational demand.

Typically, the regularized ML estimation (or MAP) [15, 16, 24, 64] is used in image restoration therefore the determination of the regularization parameter is an important issue in the image restoration. A. M. Thompson, J. C. Brown, J. W. Kay and D. M. Titterington [1] proposed the Methods of choosing the smoothing parameter in image restoration by regularized ML in 1991. Next, V. Z. Mesarovic, N. P. Galatsanos, A. K. Katsaggelos [123] proposed the single image restoration using regularized ML for unknown linear space-invariant (LSI) point spread function (PSF) in 1995. Subsequently, D. Geman and C. Yang [14] proposed single image restoration using regularized ML with robust nonlinear regularization in 1995. This approach can be done efficiently by Monte Carlo Methods, for example by annealing FFT domain using Markov chain that alternates between (global) transitions from one array to the other. Later, M. G. Kang and A. K. Katsaggelos proposed the use of a single image regularization functional [55], which is defined in terms of restored image at each iteration step, instead of a constant regularization parameter in 1995 and proposed regularized ML for SRR [56], in which no prior knowledge of the noise variance at each frame or the degree of smoothness of the original image is required in 1997. In 1999, R. Molina, A. K. Katsaggelos, and J. Mateos [85] proposed the application of the hierarchical ML with Laplacian regularization to the single image restoration problem and derived expressions for the iterative evaluation of the two hyperparameters (regularized parameter) applying the evidence and maximum a posteriori (MAP) analysis within the hierarchical regularized ML paradigm. In 2003, R. Molina, M. Vega, J. Abad and A. K. Katsaggelos [86] proposed the mutiframe super-resolution reconstruction using ML with Laplacian regularization. The regularized parameter is defined in terms of restored image at each iteration step. Next, D. Rajan and S. Chaudhuri [21] proposed super-resolution approach, based on ML with MRF regularization, to simultaneously estimate the depth map and the focused image of a scene, both at a super-resolution from its defocused observed images in 2003. Subsequently, H. He and L. P. Kondi [29-30] proposed image resolution enhancement with adaptively weighted low-resolution images (channels) and simultaneous estimation of the regularization parameter in 2004 and proposed a generalized framework [31] of regularized image/video Iterative Blind Deconvolution/Super-Resolution (IBD-SR) algorithm using some information from the more matured blind Deconvolution techniques form image restoration in 2005. Later, they [32] proposed SRR algorithm that takes into account inaccurate estimates of the registration parameters and the point spread function in 2006. In 2006, M. Vega, R. Molina and A. K. Katsaggelos [67] proposed the problem of deconvolving color images observed with a single coupled charged device (CCD) from the super-resolution point of view. Utilizing the regularized ML paradigm, an estimate of the reconstructed image and the model parameters is generated.

M. Elad and A. Feuer [49] proposed the hybrid method combining the ML and nonellipsoid constraints for the super-resolution restoration in 1997 and the adaptive filtering approach for the Super-Resolution Reconstruction in 1999 [50, 51]. Next, they proposed two iterative algorithms, the R-SD and the R-LMS [51], to generate the desired image sequence at the practically computational complexity in 1999. These algorithms assume the knowledge of the blur, the down-sampling, the sequences motion, and the measurements noise characteristics, and apply a sequential reconstruction process. Subsequently, the special case of Super-Resolution Reconstruction (where the warps are pure translations, the blur is space

invariant and the same for all the images and the noise is white) are proposed for a fast Super-Resolution Reconstruction in 2001 [52]. Later, N. Nguyen, P. Milanfar and G. Golub [70] proposed fast SRR algorithm using regularized ML by using efficient block circulant preconditioners and the conjugate gradient method in 2001. In 2002, M. Elad [54] proposed the Bilateral Filter theory, showed how the bilateral filter can be improved and extended to treat more general reconstruction problems. Consequently, the alternate super-resolution approach, L1 Norm estimator and robust regularization based on a Bilateral Total Variance (BTV), was presented by S. Farsiu and D. Robinson [97-98] in 2004. This approach performance is superior to what proposed earlier in [49], [50] and [51] and this approach has fast convergence but this SRR algorithm effectively apply only on AWGN models. Next, they proposed a fast SRR of color images [99] using ML estimator with BTV regularization for luminance component and Tikhonov regularization for chrominance component in 2006. Subsequently, they proposed the dynamic super-resolution problem of reconstructing a highquality set of monochromatic or color super-resolved images from low-quality monochromatic, color or mosaiced frames [100]. This approach includes a joint method for simultaneous SR, deblurring and Demosaicing. It takes into account practical color measurements encountered in video sequences. Later, we [112] proposed the SRR using a regularized ML estimator with affine block-based registration for the real image sequence. Moreover, G. Rochefort, F. Champagnat, G. L. Besnerais and Jean-François Giovannelli [25] proposed super-resolution approach based on regularized ML [49] for the extended original observation model devoted to the case of nonisometire I nterframe motion such as affine motion in 2006.

S. Baker and T. Kanade [92] proposed another super-resolution algorithm (hallucination or recognition-based super-resolution) in 2002 that attempts to recognize local features in the low-resolution image and then enhances their resolution in an appropriate manner. Due to the training data base, therefore, this algorithm performance depends on the image type (such as face or character) and this algorithm is not robust enough to be sued in typical surveillance video. J. Sun, N. N. Zheng, H. Tao and H. Y. Shum [41] proposed hallucination super-resolution (for single image) using regularization ML with primal sketches as the basic recognition elements in 2003.

During 2004 to 2006, P. Vandewalle, S. Susstrunk and M. Vetterli [75-78] have proposed a fast super-resolution reconstruction based on a non-uniform interpolation using a frequency domain registration. This method has low computation and can use in the real-time system but the degradation models are limited therefore this algorithm can apply on few applications. In 2006, M. Trimeche, R. C. Bilcu and J. Yrjanainen [65] proposed SRR algorithm using an integrated adaptive filtering method to reject the outlier image regions for which registration has failed.

1.2.1 SSR Estimation Technique Problem

This section reviews the literature from the estimation point of view because the SRR estimation is one of the most crucial parts of the SRR research areas and directly impact to the SRR performance. Though the SRR algorithms from the reviews literature use various techniques, there are only two kinds of norm estimation (L1 and L2). L2 norm estimation has the advantage of lower variance than the L1 norm; whereas, L1 performs better in robust to outliers because the influence function is constant and bounded.

C. Bouman and K. Sauer [10] proposed the single image restoration algorithm using ML estimator (L2 Norm) with the GGMRF (Generalized Gaussian-Markov Random

Field) regularization in 1993. R. R. Schultz and R. L. Stevenson [88] proposed the single image restoration algorithm using ML estimator (L2 Norm) with the HMRF (Huber-Markov Random Field) regularization in 1994 and proposed the SRR algorithm [89] using ML estimator (L2 Norm) with the HMRF regularization in 1996. The blur of the measured images is assumed to be simple averaging and the measurements additive noise is assumed to be independent and identically distributed (i.i.d.) Gaussian vector. M. Elad and A. Feuer [49] proposed the hybrid method combining the ML estimator (L2 Norm) and nonellipsoid constraints for the Super-Resolution Reconstruction in 1997 [50]. Next, they proposed two iterative algorithms, the R-SD and the R-LMS (L2 Norm) [50, 53], to generate the desired image sequence at the practically computational complexity in 1999. These algorithms assume the knowledge of the blur, the down-sampling, the sequences motion, and the measurements noise characteristics, and apply a sequential reconstruction process. Subsequently, the special case of Super-Resolution Reconstruction (where the warps are pure translations, the blur is space invariant and the same for all the images and the noise is white) are proposed for a fast Super-Resolution Reconstruction using ML estimator (L2 Norm) in 2001 [52]. Later, N. Nguyen, P. Milanfar and G. Golub [70] proposed fast SRR algorithm using regularized ML (L2 Norm) by using efficient block circulant preconditioners and the conjugate gradient method in 2001. In 2002, A. J. Patti and Y. Altunbasak proposed [2] a SRR algorithm using ML (L2 Norm) estimator with POCS-based regularization. Y. Altunbasak, A. J. Patti, and R. M. Mersereau [126] proposed a SRR algorithm using ML (L2 Norm) estimator for the MPEG sequences in 2002. Deepu Rajan and S. Chaudhuri [21] proposed SRR using ML (L2 Norm) with MRF regularization to simultaneously estimate the depth map and the focused image of a scene in 2003. Later, we [112] proposed the SRR using a regularized ML estimator (L2 Norm) with affine block-based registration for the real image sequence. Moreover, G. Rochefort, F. Champagnat, G. L. Besnerais and Jean-Francois Giovannelli [25] proposed super-resolution approach based on regularized ML (L2 Norm) [49] for the extended original observation model devoted to the case of nonisometirc Interframe motion such as affine motion in 2006. In 2006, R. Pan and S. J. Reeves [87] proposed single image restoration algorithm using ML estimator (L2 Norm) with the efficient HMRF regularization and using decomposition-enabled edge-preserving image restoration in order to reduce the computational demand.

The novel super-resolution approach, ML estimator (L1 Norm) and robust regularization based on a Bilateral Total Variance (BTV), was presented by S. Farsiu and D. Robinson [97-98] in 2004. Next, they proposed a fast SRR of color images [99] using ML estimator (L1 Norm) with BTV regularization for luminance component and Tikhonov regularization for chrominance component in 2006. Subsequently, they proposed the dynamic super-resolution problem of reconstructing a high-quality set of monochromatic or color super-resolved images from low-quality monochromatic, color or mosaiced frames [100]. This approach includes a joint method for simultaneous SR, deblurring and Demosaicing, this way taking into account practical color measurements encountered in video sequences.

The success of SRR algorithm is highly dependent on the accuracy of the model of the imaging process. However, these models are not supposed to be exactly true, as they are merely mathematically convenient formulations of some general prior information. When the data or noise model assumptions do not faithfully describe the measure data, the estimator performance degrades rapidly. Furthermore, existence of outliers defined as data points with different distributional characteristics than the assumed model will produce erroneous estimates. Most of noise models used in SRR algorithms is based on AWGN (Additive White Gaussian Noise) model; therefore, SRR algorithms can effectively apply only on the image sequence that is corrupted by AWGN. Due to this noise model, L1 norm or L2 norm error are effectively used in SRR algorithm. Unfortunately, the real noise models that corrupt the measure sequence are unknown therefore SRR algorithm using L1 norm or L2

norm may degrade the image sequence rather than enhance it. Therefore, the robust norm error is desired for SRR algorithm. This norm should be strong against several noise models. For normally distributed data, the L1 norm produces estimates with higher variance than the optimal L2 (quadratic) norm but the L2 norm is very sensitive to outliers because the influence function increases linearly and without bound.

2. FUNDAMENTAL TECHIQUES FOR SUPER-RESOLUTION RECONSTRUCTION

2.1 METHODOLOGY: SUPER RESOLUTION RECONSTRUCTION ALGORITHM

2.1.1 Super-Resolution Reconstruction as an Ill-Posed Inverse Problem

In SRR, typically, the LR images represent different "looks" at the same scene [95]. That is, LR images are subsampled (aliased) as well as shifted with sub-pixel precision. If the LR images are shifted by integer units, then each image contains the same information, and thus there is no new information that can be used to reconstruct a HR image. If the LR images have different sub-pixel shifts from each other and aliasing is present, however, then each image cannot be obtained from others. In this case, the new information contained in each LR image can be exploited to obtain a HR image. To obtain different looks at the same scene, some relative scene motions must exist from frame to frame via multiple scenes or video sequences. Multiple scenes can be obtained from one camera with several captures or from multiple cameras located in different positions. These scene motions can occur due to the controlled motions in imaging systems, e.g., images acquired from orbiting satellites. The same is true for uncontrolled motions, e.g., movement of local objects or vibrating imaging systems. If these scene motions are known or can be estimated within sub-pixel accuracy and we combine these LR images then SRR is possible. One of the recurring issues in this work is that multiframe Super-Resolution Reconstruction is usually an ill-posed inverse problem.

2.1.1.1 Super-Resolution Reconstruction is an Inverse Problem

SRR refers to the restoration of a sequence of observed low-resolution images that has information content beyond the spatial and/or temporal bandlimit of the imaging system (bandwidth extrapolation). Hence, the corresponding inverse problem is that of determining estimate(s) of the scene given the observed image sequence and the characterization of the imaging process. Given the characteristics of the imaging process and system, the forward problem is the simulation, while the inverse problem is the restoration.

2.1.1.2 Super-Resolution Reconstruction is an III-Posed Problem

Recall that ill-posedness implies failure of one or more of the Hadamard conditions. The multiframe SRR problem may fail to satisfy one or more of these conditions. The failure may result from either the characteristics of the imaging system, or the observed data.

- 1. Nonexistence of the solution: the presence of noise in the observation process may result in an observed image sequence which, given the imaging system characterization, is inconsistent with any scene. The result is that the system is noninvertible and the scene cannot be estimated from the observations.
- 2. Nonuniqueness of the solution: when the operator which characterizes the imaging process is many-to-one, there exists a nontrivial space of solutions consistent with any given observed image sequence, that is, the solution to the inverse problem is nonunique. For example, in bandlimited imaging systems, all out-of-band scene data represent the null

space of the imaging process operator. Even if the imaging operator is nonsingular, a simple lack of data, which represent constraints on the solution space, is sufficient to result in the nonuniqueness of the solution. For example, consider a discretized imaging scenario with P observed low-resolution images each consisting of N pixels. These observed data provide a maximum of PN independent constraints. Assume a single superresolution image containing M > PN pixels is to be estimated from the data. Since the number of unknowns exceeds the number of constraints, it is clear that there are insufficient constraints for the existence of a unique solution to the inverse problem. Furthermore, since superresolution, by definition, requires the restoration of information that is lost in the imaging process it should be expected that the solution to the superresolution restoration problem is likely to be nonunique.

3. Discontinuous dependence of the solution on the data: depending on the characteristics of the imaging system, the inverse problem may be highly sensitive to perturbations of the data. For example, consider an imaging system with a spectral response which decreases asymptotically toward zero with increasing frequency. While such a system is invertible in theory, in practice the inverse is unstable. An arbitrarily small noise component at a sufficiently high frequency leads to an arbitrarily large spurious signal in the computed restoration. In practice such restorations are typically overwhelmed by the amplification of the noise.

While, in rare circumstances, it happens that the Hadamard conditions are satisfied, in general, practical applications involving multiframe SRR are invariably ill-posed. Despite the difficulties caused by the ill-posedness, regularized solution methods enable high quality SRR as is shown in later section. The inclusion of a-priori information is crucial to achieving this.

2.1.2 The Classical SRR Algorithm

In this section, the classical SRR algorithm is presented. First, the SRR observation model is described and, consequently, the classical regularized ML for the SRR algorithm is stated.

2.1.2.1 The SRR Observation Model

The first step to comprehensively analyze the SRR problem is to formulate an observation model that relates the original HR image to the observed LR images. The observation models can be broadly divided into the models for still images and for video sequence. To present a basic concept of SRR algorithms, we first employ the observation model for still images and, later, we extend it to the observation model for the video sequence model.

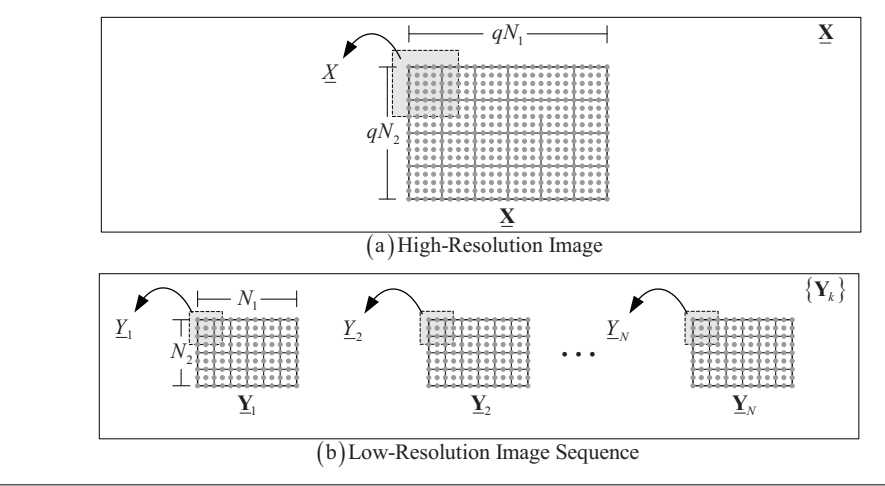
Define that a low-resolution image sequence is $\{\underline{\mathbf{Y}}_k\}$, $N_1 \times N_2$ pixels, as our measured data. A original high-resolution image $\underline{\mathbf{X}}$, $qN_1 \times qN_2$ pixels, is to be estimated from the LR sequences, where q is an integer-valued interpolation factor in both the horizontal and vertical directions. To reduce the computational complexity, each frame is separated into overlapping blocks (the shadow blocks as shown in Fig. 5.1(a) and Fig. 5.1(b)).

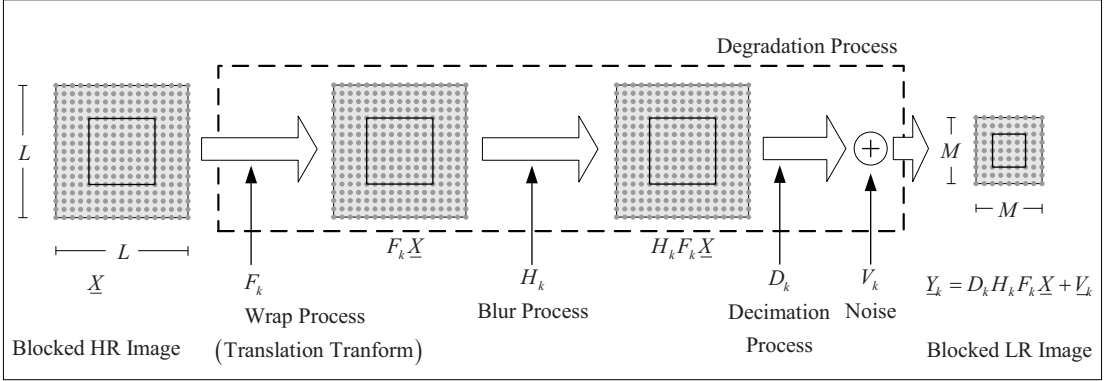
For convenience of notation, all overlapping blocked frames will be presented as vector, ordered column-wise lexicographically. Namely, the overlapping blocked LR frame is $\underline{Y}_k \in \mathbb{R}^{M^2}$ $(M^2 \times 1)$ and the overlapping blocked HR frame is $\underline{X} \in \mathbb{R}^{q^2M^2}$ $(L^2 \times 1 \text{ or } q^2M^2 \times 1)$. We assume that the two images are related via the following equation

$$\underline{Y}_{k} = D_{k} H_{k} F_{k} \underline{X} + V_{k} \quad ; k = 1, 2, ..., N$$
 (2.1)

where

- X (vector format) is the original high-resolution blocked image.
- $\underline{Y}_k(t)$ (vector format) is the blurred, decimated, down sampled and noisy blocked image
- F_k $(F \in \mathbb{R}^{q^2M^2 \times q^2M^2})$ and matrix format) stands for the geometric warp (Typically, Translational Motion) between the images \underline{X} and \underline{Y}_k .
- H_k ($H_k \in \mathbb{R}^{q^2M^2 \times q^2M^2}$ and matrix format) is the blur matrix which is a space and time invariant.
- D_k ($D_k \in \mathbb{R}^{M^2 \times q^2 M^2}$ and matrix format) is the decimation matrix assumed constant.
- V_k ($V_k \in \mathbb{R}^{M^2}$ and vector format) is a system noise.





(c) The Relation between Overlapping Blocked HR Image and Overlapping Blocked LR Image Sequence (SRR Observation Model)

Figure 2.2 The Classical SRR Observation Model

2.1.2.2 The Classical Regularized ML for SRR Algorithm

A popular family of estimators is the ML-type estimators (M estimators) [50, 70]. We rewrite the definition of these estimators in the super resolution reconstruction framework as the following minimization problem:

$$\underline{\hat{X}} = \operatorname{ArgMin} \left\{ \sum_{k=1}^{N} \rho \left(D_k H_k F_k \underline{X} - \underline{Y}_k \right) \right\}$$
(2.2)

where $\rho(\cdot)$ is a norm estimation. To minimize (2.2), the intensity at each pixel of the expected image must be close to those of the original image.

SRR (Super-Resolution Reconstruction), described in Section 5.1, is an ill-posed problem [98]. For the under-determined cases (i.e., when fewer than required frames are available), there exist an infinite number of solutions which satisfy (2.2). The solution for squared and over-determined cases is not stable, which means small amounts of noise in measurements will result in large perturbations in the final solution. Therefore, considering regularization in SRR algorithm as a mean for picking a stable solution is very useful, if not necessary. Also, regularization can help the algorithm to remove artifacts from the final answer and improve the rate of convergence. A regularization term compensates the missing measurement information with some general prior information about the desirable HR solution, and is usually implemented as a penalty factor in the generalized minimization cost function. Unfortunately, certain types of regularization cost functions work efficiently for some special types of images but are not suitable for general images.

2.1.2.3 L2 Norm Estimation with Laplacian Regularization for SRR Algorithm [98-100]

By using L2 norm estimation, we rewrite the definition of these estimators in the super resolution context as the following minimization problem:

$$\underline{X} = \operatorname{ArgMin} \left\{ \sum_{k=1}^{N} \left(D_{k} H_{k} F_{k} \underline{X} - \underline{Y}_{k} \right)^{2} + \lambda \cdot \left(\Gamma \underline{X} \right)^{2} \right\} \tag{2.3}$$

$$\frac{\partial}{\partial \underline{X}} \left\{ \sum_{k=1}^{N} \left(D_{k} H_{k} F_{k} \underline{X} - \underline{Y}_{k} \right)^{2} + \lambda \cdot \left(\Gamma \underline{X} \right)^{2} \right\} = 0$$

$$\sum_{k=1}^{N} \left\{ \frac{\partial}{\partial \underline{X}} \left(D_{k} H_{k} F_{k} \underline{X} - \underline{Y}_{k} \right)^{2} \right\} + \frac{\partial}{\partial \underline{X}} \lambda \cdot \left(\Gamma \underline{X} \right)^{2} = 0$$

$$\sum_{k=1}^{N} \left\{ F_{k}^{T} H_{k}^{T} D_{k}^{T} \left(D_{k} H_{k} F_{k} \underline{X} - \underline{Y}_{k} \right) \right\} + \Gamma^{T} \cdot \lambda \cdot \left(\Gamma \underline{X} \right) = 0$$

$$\sum_{k=1}^{N} \left\{ F_{k}^{T} H_{k}^{T} D_{k}^{T} \left(D_{k} H_{k} F_{k} \underline{X} - \underline{Y}_{k} \right) \right\} + \lambda \cdot \left(\Gamma^{T} \Gamma \underline{X} \right) = 0$$

$$\left(\sum_{k=1}^{N} F_{k}^{T} H_{k}^{T} D_{k}^{T} \underline{Y}_{k} \right) - \left(\sum_{k=1}^{N} F_{k}^{T} H_{k}^{T} D_{k}^{T} D_{k} H_{k} F_{k} \right) + \lambda \cdot \left(\Gamma^{T} \Gamma \right) \underline{X} = 0$$

$$\left(\sum_{k=1}^{N} F_{k}^{T} H_{k}^{T} D_{k}^{T} \underline{Y}_{k} \right) - \left(\left(\sum_{k=1}^{N} F_{k}^{T} H_{k}^{T} D_{k}^{T} D_{k} H_{k} F_{k} \right) + \lambda \cdot \left(\Gamma^{T} \Gamma \right) \underline{X} = 0$$

$$\left(\sum_{k=1}^{N} F_{k}^{T} H_{k}^{T} D_{k}^{T} \underline{Y}_{k} \right) - \left(\left(\sum_{k=1}^{N} F_{k}^{T} H_{k}^{T} D_{k}^{T} D_{k} H_{k} F_{k} \right) + \lambda \cdot \left(\Gamma^{T} \Gamma \right) \underline{X} = 0$$

$$\left(\sum_{k=1}^{N} F_{k}^{T} H_{k}^{T} D_{k}^{T} \underline{Y}_{k} \right) - \left(\left(\sum_{k=1}^{N} F_{k}^{T} H_{k}^{T} D_{k}^{T} D_{k} H_{k} F_{k} \right) + \lambda \cdot \left(\Gamma^{T} \Gamma \right) \underline{X} = 0$$

By the steepest descent method, the solution of above Equation is defined as

$$\frac{\hat{X}_{n+1}}{\hat{X}_{n+1}} = \frac{\hat{X}_{n}}{\hat{X}_{n}} + \beta \cdot \left(\sum_{k=1}^{N} F_{k}^{T} H_{k}^{T} D_{k}^{T} \underline{Y}_{k} \right) - \left(\left(\sum_{k=1}^{N} F_{k}^{T} H_{k}^{T} D_{k}^{T} D_{k} H_{k} F_{k} \right) + \lambda \cdot \left(\Gamma^{T} \Gamma \right) \right) \hat{\underline{X}}_{n} \right)$$

$$\frac{\hat{X}_{n+1}}{\hat{X}_{n+1}} = \frac{\hat{X}_{n}}{\hat{X}_{n}} + \beta \cdot \left(\left(\sum_{k=1}^{N} F_{k}^{T} H_{k}^{T} D_{k}^{T} \underline{Y}_{k} \right) - \left(\left(\sum_{k=1}^{N} F_{k}^{T} H_{k}^{T} D_{k}^{T} D_{k} H_{k} F_{k} \right) + \lambda \cdot \left(\Gamma^{T} \Gamma \right) \right) \hat{\underline{X}}_{n} \right)$$

$$\frac{\hat{X}_{n+1}}{\hat{X}_{n+1}} = \frac{\hat{X}_{n}}{\hat{X}_{n}} + \beta \cdot \left\{ \left(\sum_{k=1}^{N} F_{k}^{T} H_{k}^{T} D_{k}^{T} \left(\underline{Y}_{k} - D_{k} H_{k} F_{k} \underline{\hat{X}}_{n} \right) - \left(\lambda \cdot \left(\Gamma^{T} \Gamma \right) \underline{\hat{X}}_{n} \right) \right\} \tag{2.4}$$

 $\mathbf{P} - \mathbf{R}X = 0$

2.1.2.4 L1 Norm Estimation with Laplacian Regularization for SRR Algorithm [98-100]

By using L1 norm estimation, the definition of these estimators in the super resolution context is rewritten as the following minimization problem:

$$\underline{X} = \operatorname{ArgMin} \left\{ \sum_{k=1}^{N} \left| D_{k} H_{k} F_{k} \underline{X} - \underline{Y}_{k} \right| + \lambda \cdot \left(\Gamma \underline{X} \right)^{2} \right\}$$

$$\frac{\partial}{\partial \underline{X}} \left\{ \sum_{k=1}^{N} \left\| D_{k} H_{k} F_{k} \underline{X} - \underline{Y}_{k} \right\|_{1} + \lambda \cdot \left(\Gamma \underline{X} \right)^{2} \right\} = 0$$

$$\sum_{k=1}^{N} \left\{ \frac{\partial}{\partial \underline{X}} \left\| D_{k} H_{k} F_{k} \underline{X} - \underline{Y}_{k} \right\|_{1} \right\} + \frac{\partial}{\partial \underline{X}} \lambda \cdot \left(\Gamma \underline{X} \right)^{2} = 0$$
(2.5)

By the steepest descent method, the solution of Equation (2.5) is defined as

$$\underline{\hat{X}}_{n+1} = \underline{\hat{X}}_n + \beta \cdot \left\{ \left(\sum_{k=1}^N F_k^T H_k^T D_k^T \operatorname{sign} \left(D_k H_k F_k \underline{\hat{X}}_n - \underline{Y}_k \right) \right) - \left(\lambda \cdot \left(\Gamma^T \Gamma \right) \underline{\hat{X}}_n \right) \right\}$$
(2.6)

2.1.2.5 L2 Norm Estimation with MRF Regularization for SRR Algorithm [87-89]

By using L2 norm estimation, the definition of these estimators in the super resolution context is defined as the following minimization problem:

$$\underline{X} = \operatorname{ArgMin} \left\{ \sum_{k=1}^{N} \left(\left(D_{k} \cdot H_{k} \cdot F_{k} \cdot \underline{X} - \underline{Y}_{k} \right)^{2} \right) + \left(-\frac{1}{2\beta_{MRF}} \sum_{c \in C} \rho_{\alpha} \left(\mathbf{d}_{c}^{t} \underline{X} \right) \right) \right\} \tag{2.7}$$

$$\frac{\partial}{\partial \underline{X}} \left\{ \sum_{k=1}^{N} \left\| D_{k} H_{k} F_{k} \underline{X} - \underline{Y}_{k} \right\|_{2}^{2} + \left(-\frac{1}{2\beta_{MRF}} \sum_{c \in C} \rho_{\alpha} \left(\mathbf{d}_{c}^{t} \underline{X} \right) \right) \right\} = 0$$

$$\frac{\partial}{\partial \underline{X}} \left\{ \sum_{k=1}^{N} \left\| D_{k} H_{k} F_{k} \underline{X} - \underline{Y}_{k} \right\|_{2}^{2} \right\} + \frac{\partial}{\partial \underline{X}} \left(-\frac{1}{2\beta_{MRF}} \sum_{c \in C} \left(\mathbf{d}_{c}^{t} \underline{X} \right)^{2} \right) = 0$$

$$\frac{\partial}{\partial \underline{X}} \left\{ \sum_{k=1}^{N} \left\| D_{k} H_{k} F_{k} \underline{X} - \underline{Y}_{k} \right\|_{2}^{2} \right\} + \left(\mathbf{d}_{2}^{t} \underline{X} \right)^{2} + \left(\mathbf{d}_{3}^{t} \underline{X} \right)^{2} + \left(\mathbf{d}_{4}^{t} \underline{X} \right)^{2} \right) = 0$$

$$\frac{\partial}{\partial \underline{X}} \left\{ \sum_{k=1}^{N} \left\| D_{k} H_{k} F_{k} \underline{X} - \underline{Y}_{k} \right\|_{2}^{2} \right\} + \left(\mathbf{d}_{3}^{t} \underline{X} \right)^{2} + \left(\mathbf{d}_{3}^{t} \underline{X} \right)^{2} + \left(\mathbf{d}_{4}^{t} \underline{X} \right)^{2} \right) = 0$$

$$\frac{\partial}{\partial \underline{X}} \left\{ \sum_{k=1}^{N} \left\| D_{k} H_{k} F_{k} \underline{X} - \underline{Y}_{k} \right\|_{2}^{2} \right\} + \left(\mathbf{d}_{3}^{t} \underline{X} \right) + \left(\mathbf{d}_{3}^{t} \mathbf{d}_{3}^{t} \underline{X} \right) + \left(\mathbf{d}_{4}^{t} \mathbf{d}_{4}^{t} \underline{X} \right) \right) = 0$$

$$\frac{\partial}{\partial \underline{X}} \left\{ \sum_{k=1}^{N} \left\| D_k H_k F_k \underline{X} - \underline{Y}_k \right\|_2^2 \right\} + \left(-\frac{1}{\beta_{MRF}} \left(\mathbf{d}_1^{tT} \mathbf{d}_1^t + \mathbf{d}_2^{tT} \mathbf{d}_2^t + \mathbf{d}_3^{tT} \mathbf{d}_3^t + \mathbf{d}_4^{tT} \mathbf{d}_4^t \right) \underline{X} \right) = 0$$

By the steepest descent method, the solution of Equation (2.7) is defined as

$$\underline{\hat{X}}_{n+1} = \underline{\hat{X}}_{n} + \beta \cdot \left\{ \left(\sum_{k=1}^{N} F_{k}^{T} H_{k}^{T} D_{k}^{T} \left(\underline{Y}_{k} - D_{k} H_{k} F_{k} \underline{\hat{X}}_{n} \right) \right) - \left(-\frac{1}{\beta_{MRF}} \left(\mathbf{d}_{1}^{\prime T} \mathbf{d}_{1}^{\prime} + \mathbf{d}_{2}^{\prime T} \mathbf{d}_{2}^{\prime} + \mathbf{d}_{3}^{\prime T} \mathbf{d}_{3}^{\prime} + \mathbf{d}_{4}^{\prime T} \mathbf{d}_{4}^{\prime} \right) \underline{X} \right) \right\}$$

$$\underline{\hat{X}}_{n+1} = \underline{\hat{X}}_{n} + \beta \cdot \left\{ \left(\sum_{k=1}^{N} F_{k}^{T} H_{k}^{T} D_{k}^{T} \left(\underline{Y}_{k} - D_{k} H_{k} F_{k} \underline{\hat{X}}_{n} \right) \right) + \left(\frac{1}{\beta_{MRF}} \left(\mathbf{d}_{1}^{\prime T} \mathbf{d}_{1}^{\prime} + \mathbf{d}_{2}^{\prime T} \mathbf{d}_{2}^{\prime} + \mathbf{d}_{3}^{\prime T} \mathbf{d}_{3}^{\prime} + \mathbf{d}_{4}^{\prime T} \mathbf{d}_{4}^{\prime} \right) \underline{X} \right) \right\}$$

$$\underline{\hat{X}}_{n+1} = \underline{\hat{X}}_{n} + \beta \cdot \left\{ \left(\sum_{k=1}^{N} F_{k}^{T} H_{k}^{T} D_{k}^{T} \left(\underline{Y}_{k} - D_{k} H_{k} F_{k} \underline{\hat{X}}_{n} \right) \right) - \left(\lambda \cdot \sum_{c \in C} \rho_{\alpha}' \left(\mathbf{d}_{c}' \underline{\hat{X}}_{n} \right) \right) \right\}$$
(2.8)

where $\rho'_{\alpha}(\cdot)$ is defined as

$$\rho_{\alpha}'(\cdot) = 2x$$
 ; if $\rho_{\alpha}(\cdot)$ is a quadratic function (2.9a)

$$\rho_{\alpha}'(\cdot) = \begin{cases} 2x & ; |x| \le T_{HUBER} \\ 2T_{HUBER} \cdot \text{sign}(x) & ; |x| > T_{HUBER} \end{cases} ; if \ \rho_{\alpha}(\cdot) \text{ is a Huber function}$$
(2.9b)

2.1.2.6 L1 Norm Estimation with MRF Regularization for SRR Algorithm [87-89]

By using L1 norm estimation, the definition of these estimators in the super resolution context is defined s the following minimization problem:

$$\underline{X} = \operatorname{ArgMin} \left\{ \sum_{k=1}^{N} \left| D_{k} \cdot H_{k} \cdot F_{k} \cdot \underline{X} - \underline{Y}_{k} \right| + \left(-\frac{1}{2\beta_{MRF}} \sum_{c \in C} \rho_{\alpha} \left(\mathbf{d}_{c}^{t} \underline{X} \right) \right) \right\} \quad (2.10)$$

$$\frac{\partial}{\partial \underline{X}} \left\{ \sum_{k=1}^{N} \left\| D_{k} H_{k} F_{k} \underline{X} - \underline{Y}_{k} \right\|_{1} + \left(-\frac{1}{2\beta_{MRF}} \sum_{c \in C} \rho_{\alpha} \left(\mathbf{d}_{c}^{t} \underline{X} \right) \right) \right\} = 0$$

$$\frac{\partial}{\partial \underline{X}} \left\{ \sum_{k=1}^{N} \left\| D_{k} H_{k} F_{k} \underline{X} - \underline{Y}_{k} \right\|_{1} \right\} + \frac{\partial}{\partial \underline{X}} \left(-\frac{1}{2\beta_{MRF}} \sum_{c \in C} \left(\mathbf{d}_{c}^{t} \underline{X} \right)^{2} \right) = 0$$

$$\begin{split} &\frac{\partial}{\partial \underline{X}} \left\{ \sum_{k=1}^{N} \left\| D_{k} H_{k} F_{k} \underline{X} - \underline{Y}_{k} \right\|_{1} \right\} \\ &+ \frac{\partial}{\partial \underline{X}} \left(-\frac{1}{2\beta_{MRF}} \left(\left(\mathbf{d}_{1}^{t} \underline{X} \right)^{2} + \left(\mathbf{d}_{2}^{t} \underline{X} \right)^{2} + \left(\mathbf{d}_{3}^{t} \underline{X} \right)^{2} + \left(\mathbf{d}_{4}^{t} \underline{X} \right)^{2} \right) \right) = 0 \\ &\frac{\partial}{\partial \underline{X}} \left\{ \sum_{k=1}^{N} \left\| D_{k} H_{k} F_{k} \underline{X} - \underline{Y}_{k} \right\|_{1} \right\} \\ &+ \left(-\frac{1}{\beta_{MRF}} \left(\left(\mathbf{d}_{1}^{tT} \mathbf{d}_{1}^{t} \underline{X} \right) + \left(\mathbf{d}_{2}^{tT} \mathbf{d}_{2}^{t} \underline{X} \right) + \left(\mathbf{d}_{3}^{tT} \mathbf{d}_{3}^{t} \underline{X} \right) + \left(\mathbf{d}_{4}^{tT} \mathbf{d}_{4}^{t} \underline{X} \right) \right) \right) = 0 \\ &\frac{\partial}{\partial \underline{X}} \left\{ \sum_{k=1}^{N} \left\| D_{k} H_{k} F_{k} \underline{X} - \underline{Y}_{k} \right\|_{1} \right\} \\ &+ \left(-\frac{1}{\beta_{MRF}} \left(\mathbf{d}_{1}^{tT} \mathbf{d}_{1}^{t} + \mathbf{d}_{2}^{tT} \mathbf{d}_{2}^{t} + \mathbf{d}_{3}^{tT} \mathbf{d}_{3}^{t} + \mathbf{d}_{4}^{tT} \mathbf{d}_{4}^{t} \right) \underline{X} \right) = 0 \end{split}$$

By the steepest descent method, the solution of Equation (2.10) is defined as

$$\frac{\hat{X}_{n+1} = \hat{X}_{n} + \beta \cdot \left\{ \left(\sum_{k=1}^{N} F_{k}^{T} H_{k}^{T} D_{k}^{T} \operatorname{sign} \left(D_{k} H_{k} F_{k} \hat{X}_{n} - \underline{Y}_{k} \right) \right) - \left(-\frac{1}{\beta_{MRF}} \left(\mathbf{d}_{1}^{tT} \mathbf{d}_{1}^{t} + \mathbf{d}_{2}^{tT} \mathbf{d}_{2}^{t} + \mathbf{d}_{3}^{tT} \mathbf{d}_{3}^{t} + \mathbf{d}_{4}^{tT} \mathbf{d}_{4}^{t} \right) \underline{X} \right) \right\}$$

$$\frac{\hat{X}_{n+1} = \hat{X}_{n} + \beta \cdot \left\{ \left(\sum_{k=1}^{N} F_{k}^{T} H_{k}^{T} D_{k}^{T} \operatorname{sign} \left(D_{k} H_{k} F_{k} \hat{X}_{n} - \underline{Y}_{k} \right) \right) + \left(\frac{1}{\beta_{MRF}} \left(\mathbf{d}_{1}^{tT} \mathbf{d}_{1}^{t} + \mathbf{d}_{2}^{tT} \mathbf{d}_{2}^{t} + \mathbf{d}_{3}^{tT} \mathbf{d}_{3}^{t} + \mathbf{d}_{4}^{tT} \mathbf{d}_{4}^{t} \right) \underline{X} \right) \right\}$$

$$\hat{X}_{n+1} = \hat{X}_{n} + \beta \cdot \left\{ \left(\sum_{k=1}^{N} F_{k}^{T} H_{k}^{T} D_{k}^{T} \operatorname{sign} \left(D_{k} H_{k} F_{k} \hat{X}_{n} - \underline{Y}_{k} \right) \right) - \left(\lambda \cdot \sum_{k=1}^{N} \rho_{\alpha}^{t} \left(\mathbf{d}_{c}^{t} \hat{X}_{n} \right) \right) \right\}$$

$$(2.11)$$

2.1.2.7 L2 Norm Estimation with BTV Regularization for SRR Algorithm [98-100]

By using L2 norm estimation, we rewrite the definition of these estimators in the super resolution context as the following minimization problem:

$$\underline{X} = \operatorname{ArgMin} \left\{ \sum_{k=1}^{N} \left(\left(D_{k} \cdot H_{k} \cdot F_{k} \cdot \underline{X} - \underline{Y}_{k} \right)^{2} \right) + \lambda \left(\sum_{l=-P}^{P} \sum_{m=0}^{P} \alpha^{|m|+|l|} \left\| \underline{X} - S_{x}^{l} S_{y}^{m} \underline{X} \right\| \right) \right\}$$
(2.12)

By the steepest descent method, the solution of Equation (12) is defined as

$$\frac{\hat{X}_{n+1} = \hat{X}_{n}}{+\beta \cdot \left\{ \left[\sum_{k=1}^{N} F_{k}^{T} H_{k}^{T} D_{k}^{T} \left(\underline{Y}_{k} - D_{k} H_{k} F_{k} \hat{\underline{X}}_{n} \right) \right] - \lambda \left(\sum_{l=-P}^{P} \sum_{m=0}^{P} \alpha^{|m|+|l|} \left(I - S_{x}^{l} S_{y}^{m} \right) \cdot \operatorname{sign} \left(\underline{\hat{X}} - S_{x}^{l} S_{y}^{m} \underline{\hat{X}} \right) \right) \right\}}$$
(2.13)

2.1.2.8 L1 Norm Estimation with BTV Regularization for SRR Algorithm [98-100]

By using L1 norm estimation, the definition of these estimators in the super resolution context is defined as the following minimization problem:

$$\underline{X} = \operatorname{ArgMin} \left\{ \begin{cases}
\sum_{k=1}^{N} \left| D_{k} \cdot H_{k} \cdot F_{k} \cdot \underline{X} - \underline{Y}_{k} \right| \\
+ \lambda \left(\sum_{l=-P}^{P} \sum_{m=0}^{P} \alpha^{|m|+|l|} \left\| \underline{X} - S_{x}^{l} S_{y}^{m} \underline{X} \right\| \right) \right\}$$
(2.14)

By the steepest descent method, the solution of Equation (15) is defined as

$$\frac{\hat{X}_{n+1} = \hat{X}_{n}}{+\beta \cdot \left\{ \left[\sum_{k=1}^{N} F_{k}^{T} H_{k}^{T} D_{k}^{T} \operatorname{sign} \left(D_{k} H_{k} F_{k} \hat{X}_{n} - \underline{Y}_{k} \right) \right] -\lambda \left(\sum_{l=-P}^{P} \sum_{m=0}^{P} \alpha^{|m|+|l|} \left(I - S_{x}^{l} S_{y}^{m} \right) \cdot \operatorname{sign} \left(\hat{X} - S_{x}^{l} S_{y}^{m} \hat{X} \right) \right) \right\}}$$
(2.15)

3. THE PROPOSED ROBUST ESTIMATION TECHNIQUES FOR SUPER RESOLUTION RECONSTRUCTION

3.1 Robust Norm Estimation for SRR [58-61]

The success of SRR algorithm is highly dependent on the accuracy of the imaging process model. Unfortunately, these models are not supposed to be exactly true, as they are merely mathematically convenient formulations of some general prior information. When the data or noise model assumptions do not faithfully describe the measure data, the estimator performance degrades. Furthermore, existence of outliers defined as data points with different distributional characteristics than the assumed model will produce erroneous estimates. Almost all noise models used in SRR algorithms are based on Additive White Gaussian Noise (AWGN) model; therefore, SRR algorithms can effectively apply only on the image sequence that is corrupted by AWGN. Due to this noise model, L1 norm or L2 norm error are effectively used in SRR algorithm. Unfortunately, the real noise models that corrupt the measure sequence are unknown therefore SRR algorithm using L1 norm or L2 norm may degrade the image sequence rather than enhance it. The robust norm error is necessary for SRR algorithm applicable to several noise models. For normally distributed data, the L1 norm produces estimates with higher variance than the optimal L2 (quadratic) norm but the L2 norm is very sensitive to outliers because the influence function increases linearly and without bound. From the robust statistical estimation [58-61], Hampel, Andrew's Sine, Geman&McClure and Leclerc Norm are designed to be more robust than L1 and L2. While these robust norms are designed to reject outliers, these norms must be more forgiving about the remaining outliers; that is, it should increase less rapidly than L2.

3.1.1 Hampel Norm Estimation for SRR

A robust estimation is estimated technique that is resistance to such outliers. In SRR framework, outliers are measured images or corrupted images that are highly inconsistent with the high resolution original image. Outliers may arise from several reasons such as procedural measurement error, noise or inaccurate mathematical model. Outliers should be investigated carefully; therefore, we need to analyze the outlier in a way which minimizes their effect on the estimated model. L2 norm estimation is highly susceptible to even a small number of discordant observations or outliers. For L2 norm estimation, the influence of the outlier is much larger than the other measured data because L2 norm estimation weights the error quadraticly. Consequently, the robustness of L2 norm estimation is poor.

Hampel's norm [58-61] is one of error norm from the robust statistic literature. It is equivalent to the L1 norm for large value. But, for normally distributed data, the L1 norm produces estimates with higher variance than the optimal L2 (quadratic) norm, so Hampel's norm is designed to be quadratic for small values and its influence does not descend all the way to zero. The Hampel norm function $(\rho(\cdot))$ and its influence function $(\rho'(\cdot))$ are shown in Figure 3.1 (a) and Figure 3.1 (b), respectively

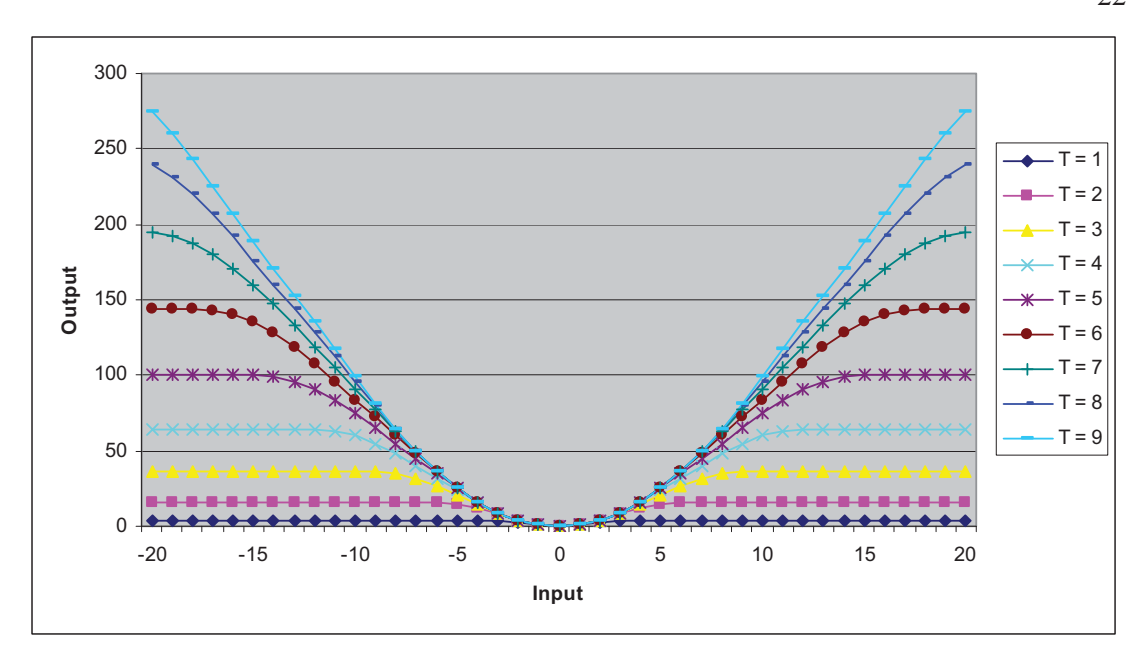


Figure 3.1 (a) The Hampel Norm function

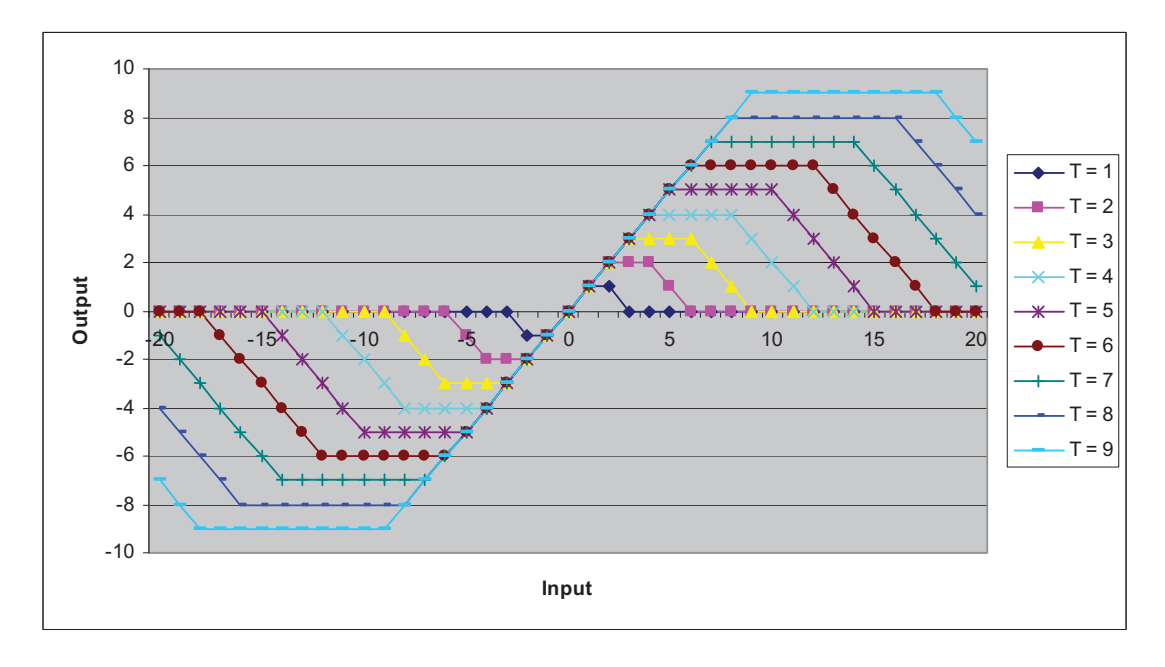


Figure 3.1 (b) The Influence function of Hampel Norm

3.1.1.1 Hampel Norm Estimation Definition

In this section, we propose the novel robust SRR using Huber error norm. From (2.2), we rewrite the definition of these robust estimators in the super resolution context as the following minimization problem:

$$\underline{X} = \operatorname{ArgMin} \left\{ \sum_{k=1}^{N} \rho_{HAMPEL} \left(D_{k} H_{k} F_{k} \underline{X} - \underline{Y}_{k} \right) \right\}$$
(3.5)

$$\rho_{HAMPEL}(x) = \begin{cases} x^{2} & ; |x| \leq T \\ 2T|x| - T^{2} & ; T < |x| \leq 2T \\ 4T^{2} - (3T - |x|)^{2} & ; 2T < |x| \leq 3T \\ 4T^{2} & ; |x| > 3T \end{cases}$$
(3.6)

where T is norm constant parameter that is a soft threshold value.

3.1.1.2 Hampel Norm Estimation for SRR

By the steepest descent method, the solution of Equation (3.5) is defined as

$$\underline{\hat{X}}_{n+1} = \underline{\hat{X}}_n + \beta \cdot \left\{ \sum_{k=1}^N F_k^T H_k^T D_k^T \cdot \rho'_{HAMPEL} \left(\underline{Y}_k - D_k H_k F_k \underline{\hat{X}}_n \right) \right\}$$
(3.7)

$$\rho'_{HAMPEL}(x) = \begin{cases} 2x & ; |x| \le T \\ 2T \operatorname{sign}(x) & ; T < |x| \le 2T \\ 2(3T - |x|) \operatorname{sign}(x) & ; 2T < |x| \le 3T \\ 0 & ; |x| > 3T \end{cases}$$
(3.8)

3.1.1.3 Hampel Norm Estimation for SRR with Laplacian Regularization [114, 115]

Combining the Laplacian regularization, we propose the solution of the super-resolution problem as follows:

$$\underline{X} = \operatorname{ArgMin} \left\{ \sum_{k=1}^{N} \rho_{HAMPEL} \left(D_{k} H_{k} F_{k} \underline{X} - \underline{Y}_{k} \right) + \lambda \cdot \left(\Gamma \underline{X} \right)^{2} \right\}$$
(3.9)

By the steepest descent method, the solution of Equation (3.9) is defined as

$$\underline{\hat{X}}_{n+1} = \underline{\hat{X}}_{n} + \beta \cdot \begin{cases}
\sum_{k=1}^{N} F_{k}^{T} H_{k}^{T} D_{k}^{T} \cdot \rho_{HAMPEL}^{\prime} \left(\underline{Y}_{k} - D_{k} H_{k} F_{k} \underline{\hat{X}}_{n} \right) \\
- \left(\lambda \cdot \left(\Gamma^{T} \Gamma \right) \underline{\hat{X}}_{n} \right)
\end{cases}$$
(3.10)

3.1.1.4 Hampel Norm Estimation for SRR with Hampel -Laplacian Regularization

Combining the Hampel-Laplacian regularization, we propose the solution of the super-resolution problem as follows:

$$\underline{X} = \operatorname{ArgMin} \left\{ \sum_{k=1}^{N} \rho_{HAMPEL} \left(D_{k} H_{k} F_{k} \underline{X} - \underline{Y}_{k} \right) + \lambda \cdot \psi_{HAMPEL} \left(\Gamma \underline{X} \right) \right\}$$
(3.11)

$$\rho'_{HAMPEL}(x) = \begin{cases} x^{2} & ; |x| \leq T_{g} \\ 2T_{g} |x| - T_{g}^{2} & ; T_{g} < |x| \leq 2T_{g} \\ 4T_{g}^{2} - (3T_{g} - |x|)^{2} & ; 2T_{g} < |x| \leq 3T_{g} \\ 4T_{g}^{2} & ; |x| > 3T_{g} \end{cases}$$
(3.12)

By the steepest descent method, the solution of Equation (3.12) is defined as

$$\underline{\hat{X}}_{n+1} = \underline{\hat{X}}_{n} + \beta \cdot \left\{ \sum_{k=1}^{N} F_{k}^{T} H_{k}^{T} D_{k}^{T} \cdot \rho_{HAMPEL}' \left(\underline{Y}_{k} - D_{k} H_{k} F_{k} \underline{\hat{X}}_{n} \right) \right\} - \left(\lambda \cdot \Gamma^{T} \cdot \psi_{HAMPEL}' \left(\Gamma \underline{\hat{X}}_{n} \right) \right)$$
(3.13)

$$\psi'_{HAMPEL} = \begin{cases} 2x & ; |x| \le T_g \\ 2T_g \operatorname{sign}(x) & ; T_g < |x| \le 2T_g \\ 2(3T_g - |x|) \operatorname{sign}(x) & ; 2T_g < |x| \le 3T_g \\ 0 & ; |x| > 3T_g \end{cases}$$
(3.14)

3.2.2 Andrew's Sine Norm Estimation for SRR

This section first reviews the main concepts of Lorentzian norm estimation technique and later develops the Lorentzian norm estimation for SRR framework.

3.2.2.1 Andrew's Sine Norm Estimation Definition

Much can be improved if the influence is bounded in one way or another. This is exactly the general idea of applying a robust error norm. Instead of using the sum of squared differences (2.6), this error norm should be selected such that above a given level of x, its influence is ruled out. In addition, one would like to have $\rho(x)$ being smooth so that numerical minimization of (2.2) is not too difficult. The one of suitable choices (among other) is so-called Andrew's Sine error norm [58-61]. In this section, we propose the novel robust SRR using Andrew's Sine error norm. From (2.2), the definition of these robust estimators in the super resolution is defined context as the following minimization problem:

$$\underline{X} = \operatorname{ArgMin} \left\{ \sum_{k=1}^{N} \rho_{ANDREW} \left(D_{k} H_{k} F_{k} \underline{X} - \underline{Y}_{k} \right) \right\}$$
(3.15)

$$\rho_{ANDREW}(x) = \begin{cases} \left(T^2\right)\sin^2\left(x/2T\right) & ; |x| \le \pi T \\ T^2 & ; |x| > \pi T \end{cases}$$
(3.16)

For values of x smaller than T, the function follows the L2 norm. For values larger than T, the function gets saturated. Consequently for small value of x, the derivative of $\rho'(x) = \partial \left\{ \rho(x) \right\} / \partial x$ of $\rho(x)$ is nearly a constant. But for large values of x (for outliers), it becomes nearly zero. Therefore, in a Gauss-Newton style of optimization, the Jacobian matrix is virtually zero for outliers. Only residuals that are about as large as T or smaller than that play a role.

From L1 and L2 norm estimation point of view, Andrew's Sine norm is equivalent to the L1 norm for large value. But, for normally distributed data, the L1 norm produces estimates with higher variance than the optimal L2 (quadratic) norm, so Andrew's Sine norm is designed to be quadratic for small values and be bound for large values. The Andrew's Sine norm function ($\rho(\cdot)$) and it influence function ($\rho'(\cdot)$) are shown in Figure 3.3 (c-1) and Figure 3.3 (c-2) respectively.

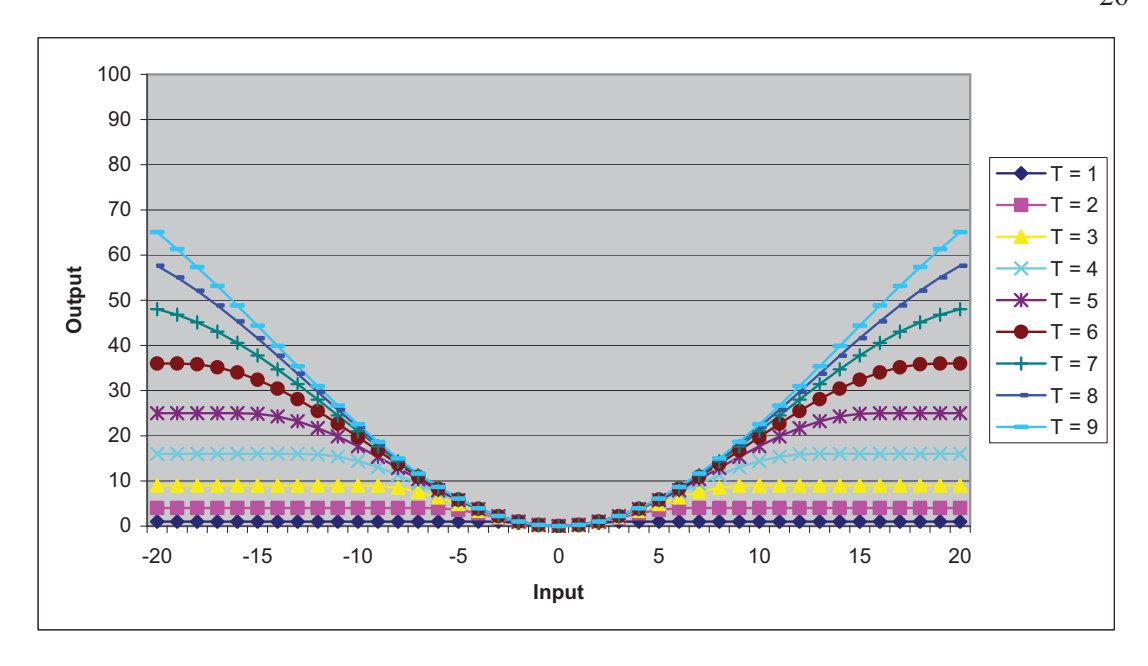


Figure 3.2 (a) The Andrew's Sine Norm function

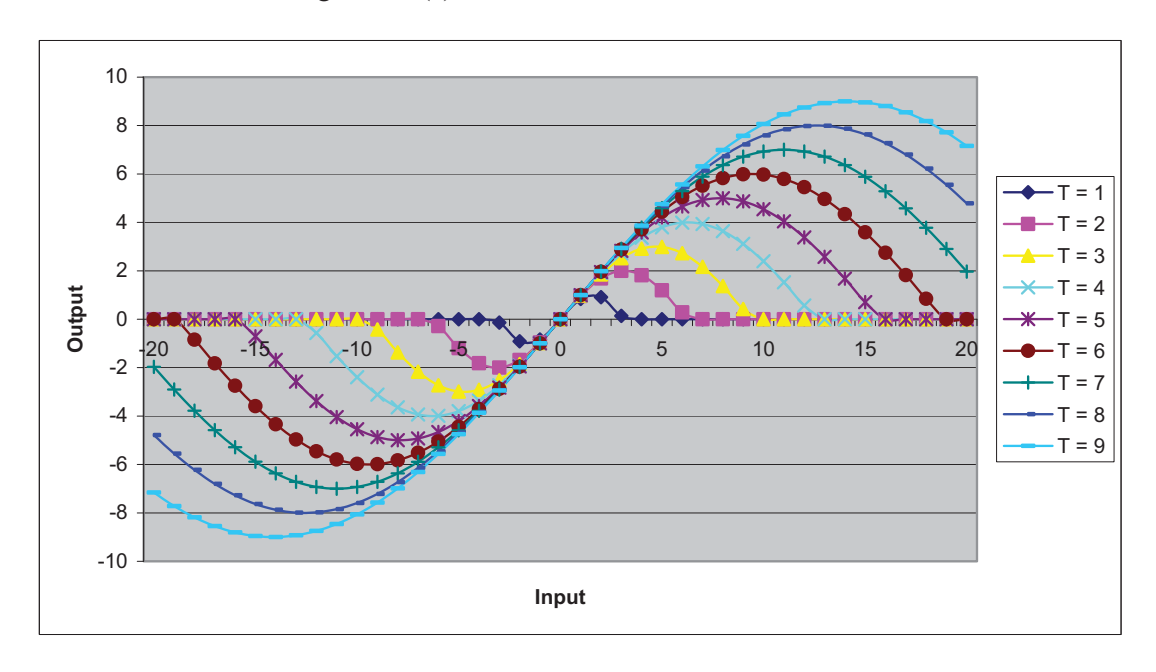


Figure 3.2 (b) The Influence function of Andrew's Sine Norm

3.2.2.2 Andrew's Sine Norm Estimation for SRR [113, 115, 116, 120]

By the steepest descent method, the solution of Equation (3.15) is defined as

$$\underline{\hat{X}}_{n+1} = \underline{\hat{X}}_n + \beta \cdot \left\{ \sum_{k=1}^N F_k^T H_k^T D_k^T \cdot \rho_{ANDREW}' \left(\underline{Y}_k - D_k H_k F_k \underline{\hat{X}}_n \right) \right\}$$
(3.17)

$$\rho_{SINE}'(x) = \begin{cases} T \sin(x/T) & ; |x| \le \pi T \\ 0 & ; |x| > \pi T \end{cases}$$
(3.18)

3.2.2.3 Andrew's Sine Norm Estimation for SRR with Laplacian Regularization [113, 115, 116, 120]

Combining the Laplacian regularization, we propose the solution of the super-resolution problem as follows:

$$\underline{X} = \operatorname{ArgMin} \left\{ \sum_{k=1}^{N} \rho_{ANDREW} \left(D_{k} H_{k} F_{k} \underline{X} - \underline{Y}_{k} \right) + \lambda \cdot \left(\Gamma \underline{X} \right)^{2} \right\}$$
(3.19)

By the steepest descent method, the solution of Equation (3.19) is defined as

$$\underline{\hat{X}}_{n+1} = \underline{\hat{X}}_{n} + \beta \cdot \left\{ \sum_{k=1}^{N} F_{k}^{T} H_{k}^{T} D_{k}^{T} \cdot \rho_{ANDREW}' \left(\underline{Y}_{k} - D_{k} H_{k} F_{k} \underline{\hat{X}}_{n} \right) \right\} - \left(\lambda \cdot \left(\Gamma^{T} \Gamma \right) \underline{\hat{X}}_{n} \right) \tag{3.20}$$

3.2.2.4 Andrew's Sine Norm Estimation for SRR with Andrew's Sine-Laplacian Regularization [113, 120]

Combining the Andrew's Sine-Laplacian regularization, we propose the solution of the super-resolution problem as follows:

$$\underline{X} = \operatorname{ArgMin} \left\{ \sum_{k=1}^{N} \rho_{ANDREW} \left(D_{k} H_{k} F_{k} \underline{X} - \underline{Y}_{k} \right) + \lambda \cdot \psi_{ANDREW} \left(\Gamma \underline{X} \right) \right\}$$
(3.21)

$$\psi_{ANDREW \atop SINE}(x) \begin{cases} \left(T_g^2\right) \sin^2\left(x/2T_g\right) & ; |x| \le \pi T_g \\ T^2 & ; |x| > \pi T_g \end{cases}$$
(3.22)

By the steepest descent method, the solution of Equation (3.21) is defined as

$$\underline{\hat{X}}_{n+1} = \underline{\hat{X}}_{n} + \beta \cdot \begin{cases}
\sum_{k=1}^{N} F_{k}^{T} H_{k}^{T} D_{k}^{T} \cdot \rho_{ANDREW}' \left(\underline{Y}_{k} - D_{k} H_{k} F_{k} \underline{\hat{X}}_{n} \right) \\
- \left(\lambda \cdot \Gamma^{T} \cdot \psi_{ANDREW}' \left(\Gamma \underline{\hat{X}}_{n} \right) \right)
\end{cases}$$
(3.23)

$$\psi'_{SINE}(x) = \begin{cases} T_g \sin(x/T_g) & ; |x| \le \pi T_g \\ 0 & ; |x| > \pi T_g \end{cases}$$
(3.24)

3.2.3 Geman&McClure Estimation Norm for SRR

This section first reviews the main concepts of Geman&McClure norm estimation technique and later develops the Geman&McClure norm estimation for SRR framework.

3.2.3.1 Geman&McClure Norm Estimation Definition

Geman&McClure norm [58-61] is another error norm from the robust statistic literature. It is more robust than L1 and L2 norm. We propose the novel robust SRR using Geman&McClure error norm. From (2.2), we rewrite the definition of these robust estimators in the super resolution context as the following minimization problem:

$$\underline{X} = \operatorname{ArgMin} \left\{ \sum_{k=1}^{N} \rho_{GM} \left(D_{k} H_{k} F_{k} \underline{X} - \underline{Y}_{k} \right) \right\}$$
(3.25)

$$\rho_{GM}(x) = T^2 \left(\frac{x^2}{T^2 + x^2}\right) \tag{3.26}$$

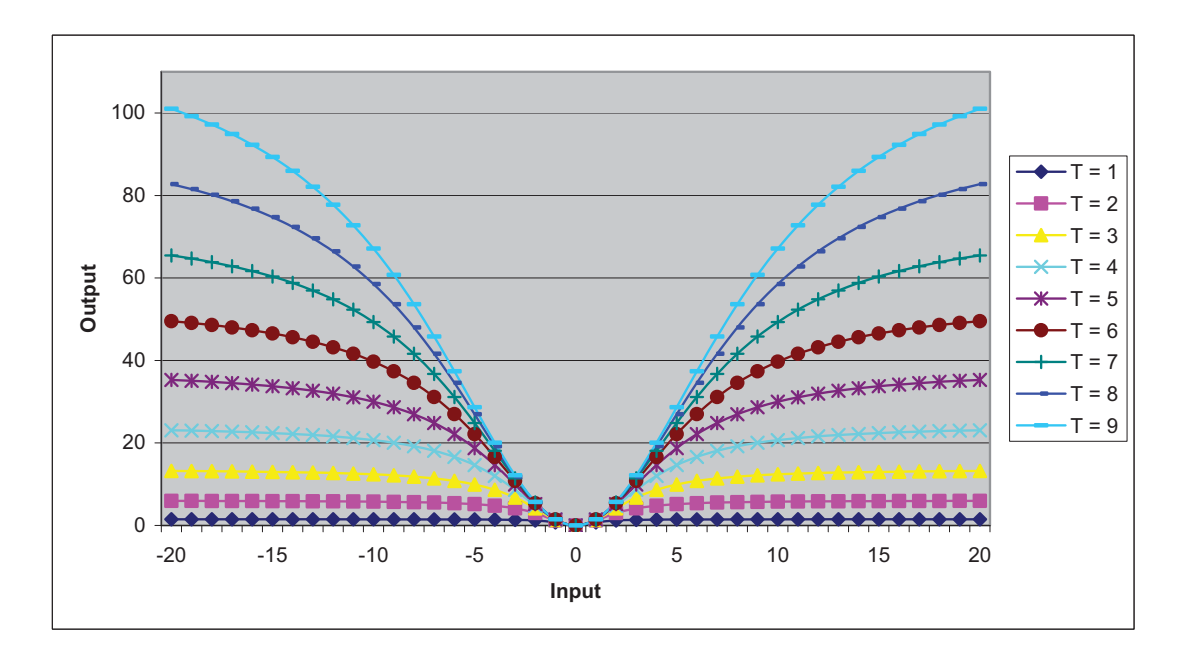


Figure 3.3 (a) The Geman&McClure Norm function

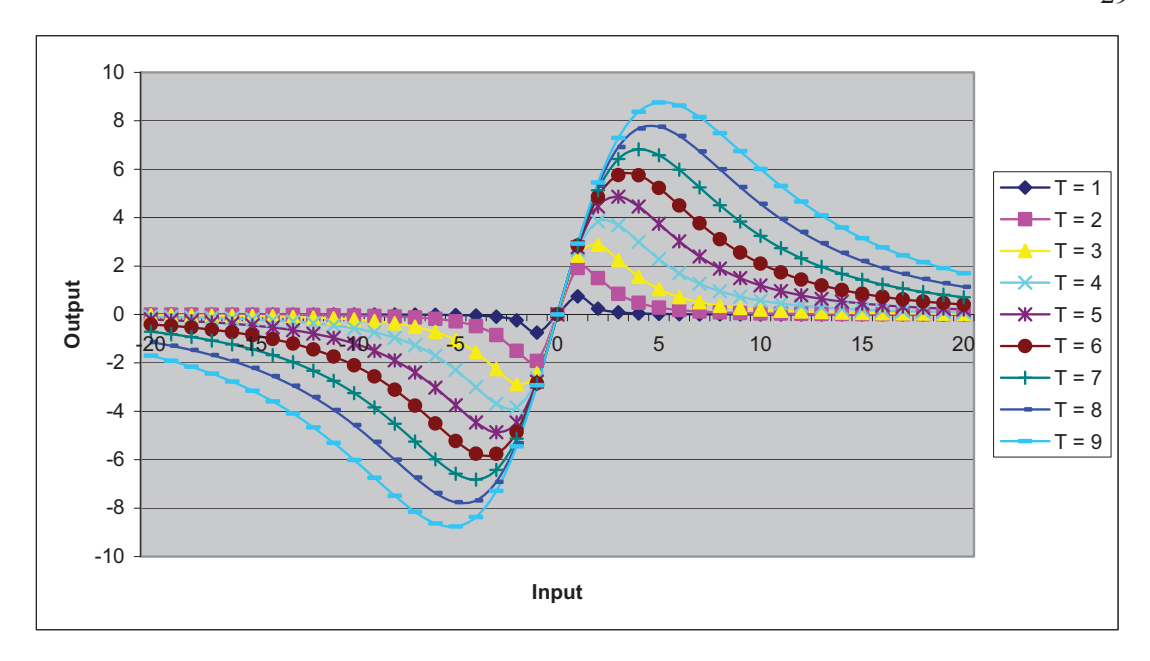


Figure 3.3 (b) The Influence function of Geman&McClure Norm

3.2.3.2 Geman&McClure Norm Estimation for SRR

By the steepest descent method, the solution of Equation (3.25) is defined as

$$\underline{\hat{X}}_{n+1} = \underline{\hat{X}}_n + \beta \cdot \left\{ \sum_{k=1}^N F_k^T H_k^T D_k^T \cdot \rho_{GM}' \left(\underline{Y}_k - D_k H_k F_k \underline{\hat{X}}_n \right) \right\}$$
(3.27)

$$\rho_{GM}'(x) = T^4 \frac{2x}{\left(T^2 + x^2\right)^2}$$
 (3.28)

3.2.3.3 Geman&McClure Norm Estimation for SRR with Laplacian Regularization

Combining the Laplacian regularization, we propose the solution of the super-resolution problem as follows:

$$\underline{X} = \operatorname{ArgMin} \left\{ \sum_{k=1}^{N} \rho_{GM} \left(D_{k} H_{k} F_{k} \underline{X} - \underline{Y}_{k} \right) + \lambda \cdot \left(\Gamma \underline{X} \right)^{2} \right\}$$
(3.29)

By the steepest descent method, the solution of Equation (3.29) is defined as

$$\underline{\hat{X}}_{n+1} = \underline{\hat{X}}_{n} + \beta \cdot \begin{cases}
\sum_{k=1}^{N} F_{k}^{T} H_{k}^{T} D_{k}^{T} \cdot \rho_{GM}' \left(\underline{Y}_{k} - D_{k} H_{k} F_{k} \underline{\hat{X}}_{n} \right) \\
- \left(\lambda \cdot \left(\Gamma^{T} \Gamma \right) \underline{\hat{X}}_{n} \right)
\end{cases}$$
(3.30)

3.2.3.4 Geman&McClure Norm Estimation for SRR with Geman&McClure Regularization

Combining the Tukey-Laplacian regularization, we propose the solution of the super-resolution problem as follows:

$$\underline{X} = \operatorname{ArgMin} \left\{ \sum_{k=1}^{N} \rho_{GM} \left(D_{k} H_{k} F_{k} \underline{X} - \underline{Y}_{k} \right) + \lambda \cdot \psi_{GM} \left(\Gamma \underline{X} \right) \right\}$$
(3.31)

$$\psi_{GM}(x) = T_g^2 \left(\frac{x^2}{T_g^2 + x^2}\right)$$
 (3.32)

By the steepest descent method, the solution of Equation (3.31) is defined as

$$\underline{\hat{X}}_{n+1} = \underline{\hat{X}}_{n} + \beta \cdot \left\{ \sum_{k=1}^{N} F_{k}^{T} H_{k}^{T} D_{k}^{T} \cdot \rho_{GM}' \left(\underline{Y}_{k} - D_{k} H_{k} F_{k} \underline{\hat{X}}_{n} \right) \right\} - \left(\lambda \cdot \Gamma^{T} \cdot \psi_{GM}' \left(\Gamma \underline{\hat{X}}_{n} \right) \right) \tag{3.33}$$

$$\psi_{GM}'(x) = T^4 \frac{2x}{\left(T^2 + x^2\right)^2}$$
 (3.34)

3.2.4 Leclerc Estimation Norm for SRR

This section first reviews the main concepts of Leclerc norm estimation technique and later develops the Leclerc norm estimation for SRR framework.

3.2.4.1 Leclerc Norm Estimation Definition

Leclerc norm [58-61] is another error norm from the robust statistic literature. It is more robust than L1 and L2 norm. While the Lorentzian norm is more robust than L2 (quadratic norm), its influence does not descend all the way to zero. Tukey's Biweight norm is a more robust from the robust statistics literature whose value does descend to zero. We propose the novel robust SRR using Tukey's Biweight error norm. From (2.2), we rewrite the definition of these robust estimators in the super resolution context as the following minimization problem:

$$\underline{X} = \operatorname{ArgMin} \left\{ \sum_{k=1}^{N} \rho_{LEC} \left(D_k H_k F_k \underline{X} - \underline{Y}_k \right) \right\}$$
(3.35)

$$\rho_{LEC}(x) = 1 - \exp\left(-\frac{x^2}{T^2}\right) \tag{3.36}$$

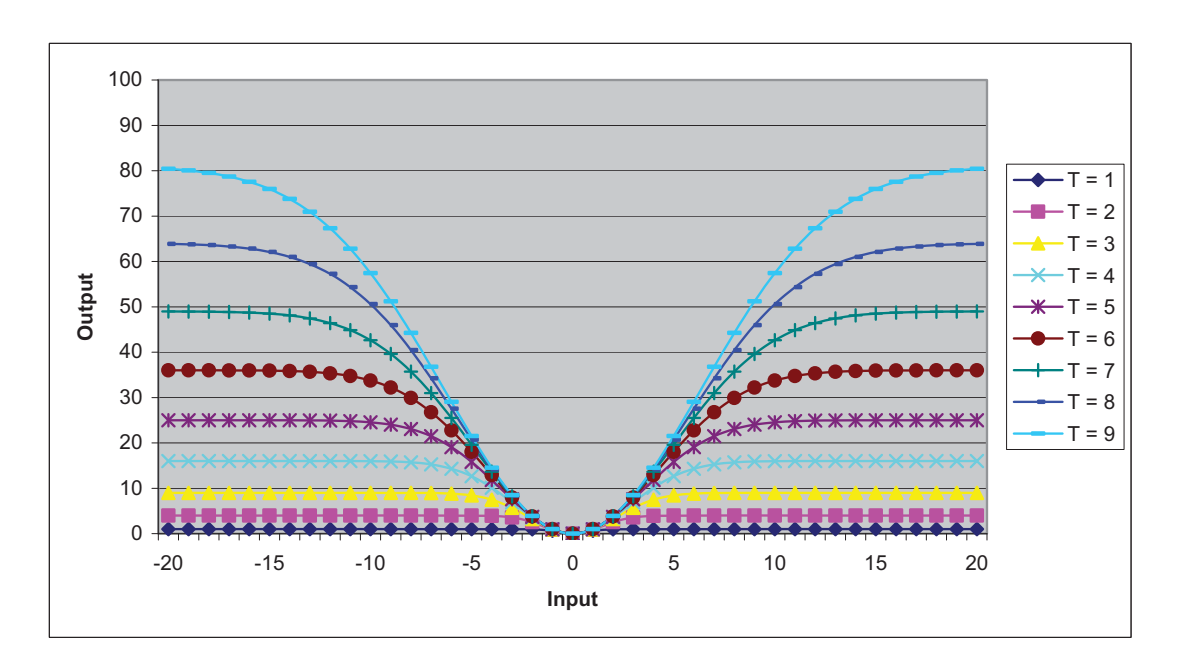


Figure 3.4 (a) The Leclerc Norm function

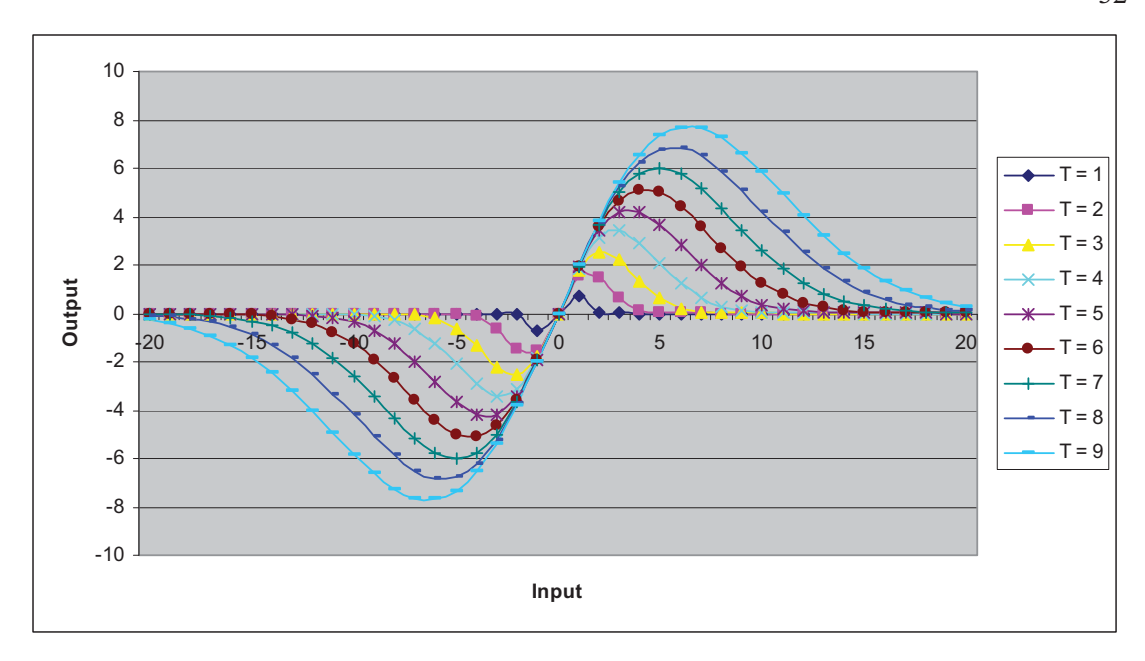


Figure 3.4 (b) The Influence function of Leclerc Norm

3.2.3.2 Leclerc Norm Estimation for SRR

By the steepest descent method, the solution of Equation (3.35) is defined as

$$\underline{\hat{X}}_{n+1} = \underline{\hat{X}}_n + \beta \cdot \left\{ \sum_{k=1}^N F_k^T H_k^T D_k^T \cdot \rho_{LEC}' \left(\underline{Y}_k - D_k H_k F_k \underline{\hat{X}}_n \right) \right\}$$
(3.37)

$$\rho_{LEC}'(x) = \left(\frac{2x}{T^2}\right) \exp\left(-\frac{x^2}{T^2}\right) \tag{3.38}$$

3.2.3.3 Leclerc Norm Estimation for SRR with Laplacian Regularization

Combining the Laplacian regularization, we propose the solution of the super-resolution problem as follows:

$$\underline{X} = \underset{X}{\operatorname{ArgMin}} \left\{ \sum_{k=1}^{N} \rho_{LEC} \left(D_{k} H_{k} F_{k} \underline{X} - \underline{Y}_{k} \right) + \lambda \cdot \left(\Gamma \underline{X} \right)^{2} \right\}$$
(3.39)

By the steepest descent method, the solution of Equation (3.29) is defined as

$$\underline{\hat{X}}_{n+1} = \underline{\hat{X}}_{n} + \beta \cdot \left\{ \sum_{k=1}^{N} F_{k}^{T} H_{k}^{T} D_{k}^{T} \cdot \rho_{LEC}^{\prime} \left(\underline{Y}_{k} - D_{k} H_{k} F_{k} \underline{\hat{X}}_{n} \right) - \left(\lambda \cdot \left(\Gamma^{T} \Gamma \right) \underline{\hat{X}}_{n} \right) \right\}$$
(3.40)

3.2.3.4 Leclerc Norm Estimation for SRR with Leclerc Regularization

Combining the Leclerc-Laplacian regularization, we propose the solution of the super-resolution problem as follows:

$$\underline{X} = \operatorname{ArgMin} \left\{ \sum_{k=1}^{N} \rho_{LEC} \left(D_{k} H_{k} F_{k} \underline{X} - \underline{Y}_{k} \right) + \lambda \cdot \psi_{LEC} \left(\Gamma \underline{X} \right) \right\}$$
(3.41)

$$\psi_{LEC}(x) = 1 - \exp\left(-\frac{x^2}{T_g^2}\right) \tag{3.42}$$

By the steepest descent method, the solution of Equation (3.41) is defined as

$$\underline{\hat{X}}_{n+1} = \underline{\hat{X}}_{n} + \beta \cdot \left\{ \sum_{k=1}^{N} F_{k}^{T} H_{k}^{T} D_{k}^{T} \cdot \rho_{LEC}' \left(\underline{Y}_{k} - D_{k} H_{k} F_{k} \underline{\hat{X}}_{n} \right) \right\} - \left(\lambda \cdot \Gamma^{T} \cdot \psi_{LEC}' \left(\Gamma \underline{\hat{X}}_{n} \right) \right) \tag{3.43}$$

$$\psi_{LEC}'(x) = \left(\frac{2x}{T_g^2}\right) \exp\left(-\frac{x^2}{T_g^2}\right)$$
(3.34)

4. THE PROPOSED IMPROVED OBSERVATION MODEL FOR SUPER RESOLUTION RECONSTRUCTION

4.1 Fast Affine Block-Based Registration/Motion Estimation [109, 112]

Almost SRR (Super-Resolution Reconstruction) algorithms reviewed in previous section are restricted to globally or locally uniform translational displacement between the measured images or sequences. This implies the measured images or sequences are observed at a high temporal frequency sampling (or high frame rate) but the measured images or sequences are usually observed by the real commercial cameras at low temporal frequency sampling (or low frame rate) such as standard sequences (Foreman, Carphone, Susie, etc.). The measured images or sequences have many complex motions instead of only a simple translational motion therefore the pure translation model can not well represent the real complex motion effectively and image super-resolution applications can apply only on the sequences that have simple translation motion.

This section proposed the novel improved SRR observation model to overcome the insufficient temporal sampling frequency and to model the real complex motion sequence that the traditional SSR observation model can not support. To realize the implementation of the proposed SRR observation model, the sub-pixel image registration is designed to calculate the nonisometric inter-frame motion parameter. Moreover, the fast algorithm is proposed to reduce the computational load for the proposed sub-pixel registration [109, 112].

This section aims to propose novel general SRR observation model (Affine Block-Based Motion Estimation) describing the complex motion more efficiently and gives excellent result on a highly accurate motion vectors in section 4.1, and to propose fast algorithm (M3SS or Modified Three Step Search) algorithm that is designed to reduce a computational load in section 4.2. This algorithm starts by partitioning the image domain into non-overlapping small regions, called blocks, and computing the motion vector within each block by an affine model, instead of a conventional translation model. Therefore, the motion vector (MV) of each block consists of six motion (instead of two) parameters.

4.1 Improved Observation Model (Affine Block-Based Registration)

Traditionally, the classical motion estimation [109, 112] can detect only pure translational motion along the image plane and fails to consider any complex motions that arise due to rotation, zooming, etc. An efficient way of detecting several complex motions is by using the combination of a block-base technique and an affine model. In this section, we propose a scheme for estimating affine block-based motion vectors suitable for several complex motions. The estimation can be separated to 2 stages. At the first stage of the estimation algorithm, the current and reference frames are divides into overlapping blocks (16x16). This stage divides the image into small areas in order to detect and estimate the local motions. The advantage of this stage is to reduce the computational load and allow the parallel processing. Next, the second stage computes the affine motion vector of each block between the current and the reference frame.

4.2 Modified Three Step Search Algorithm

The M3SS is proposed to reduce a very high computational load in affine motion vector estimation. The 3SS (Three Step Search) is one of the popular and fast algorithms used in the translational registration; therefore, this paper develops the M3SS (6

motion parameter estimation, Equation (4.1)) based on 3SS (2 motion parameter estimation Equation (4.2)).

$$mv_{x,affine}(x, y) = ax + by + c$$
 and

$$mv_{y,affine}(x,y) = dx + ey + f \tag{4.1}$$

$$mv_{x,tran}(x,y) = a$$
 and $mv_{y,tran}(x,y) = b$ (4.2)

For the 7x7 displacement window (translational deformation) and $\pm 20^{\circ}$ degree (rotation, extraction or expansion deformation), the proposed M3SS algorithm utilizes a search pattern with $3^6 = 729$ check points on a search window in the first step. The point having the minimum error is used as the center of the search area in the subsequent step. The search window is reduced by half in the subsequent step until the search window equals to pre-determined resolution. (The criterion for parameter selection in this paper was based on experiments and the chosen parameters produce the highest PSNR result on 3 standard sequences: Foreman, Carphone and Stefan [109].) The process of M3SS is described as follow:

Step 1 : Initialized the dimension of the searching area to the value depicted in Equation (4.3).

$$[a,b,c,d,e,f] = [\pm 0.16, \pm 0.16, \pm 2 \pm 0.16, \pm 0.16, \pm 2]$$
(4.3)

Step 2: A minimum BDM (Block Distortion Measure) point is found from a 729 check point pattern at the center of the searching area as shown in (4.3) and this process is shown in Fig. 4.1.

Step 3: If the search window is equal to (4.4) then the process stop otherwise go to step 4 and this process is shown in Fig. 4.2.

$$[a,b,c,d,e,f] = [\pm 0.01, \pm 0.01, \pm 0.125 \pm 0.01, \pm 0.01, \pm 0.125]$$
(4.4)

Step 4: The search window is reduced by half in all dimensions of the previous search window and a minimum BDM (Block Distortion Measure) point is found from a 729 check point pattern at the center of the new searching area. It will go to step 2.

From Table 4.1, the total number of the M3SS check points is fixed at 3.65E+3. Compared with the classical block-based estimation method (translation block-based estimation method) at 0.25 pixel accuracy and w=9, the total number of the M3SS check points has just approximately 3 times more computational load than the classical FS approach.

Table 4.1: Performance Comparison of Registration Method

Block-Based	BMA	The Number of
Registration Method	(Block Matching Algorithm)	Search Points
Affine	FS (Full Search)	1.29E+09
	M3SS	3.65E+03
Translation	FS (Full Search : 0.25 Pixel)	1.09E+03
	FS (Full Search: 1 Pixel)	2.56E+02

```
MIN_MAD = INF
For each block
    For c = -2:2:2
    For f = -2:2:2
    For a = -0.16 : 0.16 : 0.16
    For b = -0.16 : 0.16 : 0.16
    For d = -0.16 : 0.16 : 0.16
    For e = -0.16 : 0.16 : 0.16
    - The Reference frame is transformed
     by affine MV (a,b,c,d,e,f) to be
     the transformed Frame.
    - Compute the MAD value between the
     transformed frame and current frame
    - If the MAD is less than {\tt MIN\_MAD}
     then MIN_MAD is equal the MAD
     and the 1st level affine MV is
      (a,b,c,d,e,f).
    ENDfor
    ENDfor
    ENDfor
    ENDfor
    ENDfor
    ENDfor
ENDfor
```

Figure 4.1: The Algorithm of the M3SS at Step 2

```
(a_0, b_0, c_0, d_0, e_0, f_0) = \text{previous affine MV}
MIN MAD = INF
For each block
    For c = c_0 - 0.125 : 0.125 : c_0 + 0.125
    For f = f_0 - 0.125 : 0.125 : f_0 + 0.125
    For a = a_0 - 0.01 : 0.01 : a_0 + 0.01
    For b = b_0 - 0.01 : 0.01 : b_0 + 0.01
    For d = d_0 - 0.01 : 0.01 : d_0 + 0.01
    For e = e_0 - 0.01 : 0.01 : e_0 + 0.01
     - The Reference frame is transformed
      by affine MV (a,b,c,d,e,f) to be
      the transformed Frame.
     - Compute the MAD value between the
      transformed frame and current frame.
     - If the MAD is less than MIN_MAD
      then MIN_MAD is equal the MAD
      and the best affine MV is
      (a,b,c,d,e,f).
    ENDfor
    ENDfor
    ENDfor
    ENDfor
     ENDfor
     ENDfor
ENDfor
```

Figure 4.2: The Algorithm of the M3SS at Step 4

5. THE EXPERIMENTAL

The purpose of this chapter is to analyze how the proposed improved observation model (fast affine block-based) and the proposed robust norm estimation (Hampel, Andrew's Sine, Geman&McClure and Leclerc Norm) can affect the performance of the SRR algorithm.

In this chapter, three cases are studies. In the first case, Section 5.1 analyzes how the proposed robust norm estimation impacts the performance of SRR algorithm. This section presents the experiments and results obtained the SRR algorithms using the proposed robust norm estimation (Hampel, Andrew's Sine, Geman&McClure and Leclerc Norm) compared with the classical SRR algorithm using L1 and L2 norm. Section 5.2 analyzes the performance of proposed norm estimation hence this section presents the experiments and results obtained the SRR algorithms using the proposed robust norm estimation with the classical registration compared with the classical SRR algorithm using L1 and L2 norm. Finally, Section 5.3 presents the experiments and results obtained by the SRR algorithm using the proposed robust norm estimation with improved observation model (fast affine block-based).

5.1 THE EXPERIMENTAL RESULT OF PROPOSED ROBUST ESTIMATION TECHNIQUES

The purpose of this section is to analyze how the proposed robust norm estimation (Hampel, Andrew's Sine, Geman&McClure and Leclerc Norm) can affect the performance of the SRR algorithm. This section presents the experiments and results obtained the SRR algorithms using the proposed robust norm estimation (Hampel, Andrew's Sine, Geman&McClure and Leclerc Norm) compared with the classical SRR algorithm using L1 and L2 norm [113-117, 119-120].

This section presents the experiments and results obtained by the SRR algorithm methods using the proposed robust estimation (Hampel, Andrew's Sine, Geman&McClure and Leclerc Norm) with Laplacian, Hampel -Laplacian and Andrew's Sine-Laplacian, Geman&McClure-Laplacian and Leclerc-Laplacian regularization that are calculated by Equation (3.10), (3.13), (3.20), (3.23), (3.30), (3.33), (3.40) and (3.43) respectively. To demonstrate the performance of the SRR algorithm using proposed robust estimation, the results of SRR algorithm using classical L2 norm SRR with Laplacian and BTV regularization calculated by Equation (2.4) and (2.13) and the results of SRR algorithm using classical L1 norm SRR with Laplacian and BTV regularization calculated by Equation (2.8) and (2.15) are presented in order to compare the performance.

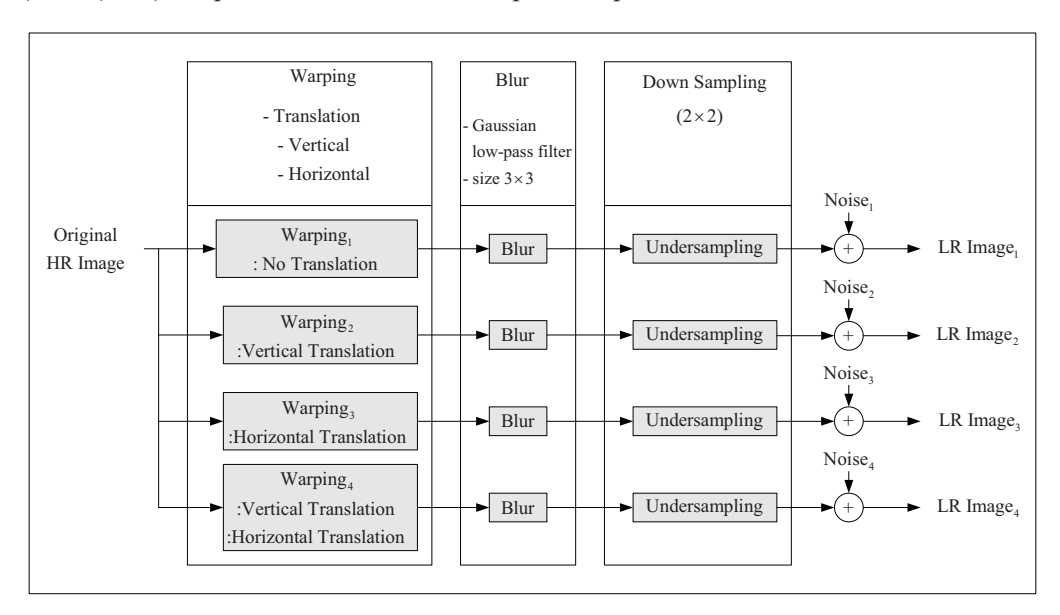


Figure 5.1: The block diagram of LR image sequence synthesis algorithm for the SRR algorithm using proposed robust estimation.

These experiments are implemented in MATLAB and the block size is fixed at 8x8 (or 16x16 for overlapping block). The 40th frame Susie sequence in QCIF format (176x144) and the Lena (Standard Image: 256x256) are used in these experiments. For the LR image sequence generation, we shifted this original HR image by a pixel in the vertical direction. Then, to simulate the effect of camera PSF, this shifted image was convolved with a symmetric Gaussian low-pass filter of the size 3x3 with the standard deviation equal to one. The resulting image was subsampled by the factor of 2 in each direction. The same approach with different motion vectors (shifts) in vertical and horizontal directions was used to produce four LR images from the original scene. We added difference noise model to the resulting LR

frames. The LR image sequence algorithm is shown in Figure 5.1. For the SRR algorithm, we use four LR frames to generate the high resolution image by the different SRR methods.

The criterion for parameter selection in this experiment was to choose parameters which produce both most visually appealing results and highest PSNR. Therefore, to ensure fairness, each experiment was repeated several times with different parameters and the best result of each experiment was chosen [97-100].

5.1.1 Experimental Result of Susie Sequence (The 40th Frame)

5.1.1.1 Noiseless

The original HR image is shown in Fig. 5.2(a-1) and one of corrupted LR images is shown in Fig. 5.2(a-2). Next, the result of implementing the SRR algorithm using L1 estimator with Laplacian Regularization, L1 estimator with BTV Regularization, L2 estimator with Laplacian Regularization, L2 estimator with BTV Regularization are shown in Figs. 5.2(a-3) - 5.2(a-6) respectively. The result of the SRR algorithm using Hampel estimator with Laplacian Regularization, Hampel estimator with Hampel-Laplacian Regularization, Andrew's Sine estimator with Laplacian Regularization, Andrew's Sine-Laplacian Regularization, Geman&McClure estimator with Laplacian Regularization, Geman&McClure-Laplacian Regularization, Leclerc estimator with Laplacian Regularization and Leclerc estimator with Leclerc-Laplacian Regularization are shown in Figs. 5.2(a-7) - 5.2(a-14) respectively.

The results indicates that Hampel, Andrew's Sine, Geman&McClure and Leclerc Norm estimator efficiently reconstruct the noiseless image than L1 and L2 estimator about 1-3 dB respectively.

5.1.1.2 AWGN (Additive White Gaussian Noise)

This experiment is a 5 AWGN cases at SNR=25, 22.5, 20, 17.5 and 15dB respectively and the original HR images are shown in Fig. 5.2(b-1) - Fig. 5.2(f-1) respectively. The corrupted images at SNR=25, 22.5, 20, 17.5 and 15dB are showed in Fig. 5.2(b-2) - Fig. 5.2(f-2) respectively.

At the high SNR (SNR=25dB, 22.5dB and 20dB) or low noise power, the L2 estimator result (with Laplacian and BTV Regularization) give slightly higher PSNR than Hampel, Andrew's Sine, Geman&McClure and Leclerc Norm estimator result. However, L2, Hampel, Andrew's Sine, Geman&McClure and Leclerc Norm estimator result have higher PSNR than L1 estimator result. At SNR=25dB, SNR=22.5dB, SNR=20dB, the result of L1 estimator with Laplacian Regularization, L1 estimator with BTV Regularization, L2 estimator with Laplacian Regularization, Hampel estimator with Laplacian Regularization, Hampel estimator with Hampel-Laplacian Regularization, Andrew's Sine estimator with Laplacian Regularization, Andrew's Sine-Laplacian Regularization, Geman&McClure estimator with Laplacian Regularization, Geman&McClure-Laplacian Regularization, Leclerc estimator with Laplacian Regularization and Leclerc estimator with Leclerc-Laplacian Regularization are shown in Fig. 5.2(b-3) - Fig. 5.2(c-3) - Fig. 5.2(c-14) and Fig. 5.2(d-3) - Fig. 5.2(d-14) respectively.

At low SNR (SNR=17.5dB and SNR=15dB) or high noise power, the Hampel, Andrew's Sine, Geman&McClure and Leclerc Norm result give the best performance than L2 estimator result (with Laplacian and BTV Regularization) and L1 estimator result (with

Laplacian and BTV Regularization). At SNR=17.5dB and SNR=15dB, the result of L1 estimator with Laplacian Regularization, L1 estimator with BTV Regularization, L2 estimator with Laplacian Regularization, L2 estimator with BTV Regularization, Hampel estimator with Laplacian Regularization, Hampel estimator with Hampel-Laplacian Regularization, Andrew's Sine estimator with Laplacian Regularization, Andrew's Sine-Laplacian Regularization, Geman&McClure estimator with Laplacian Regularization, Geman&McClure-Laplacian Regularization, Leclerc estimator with Laplacian Regularization and Leclerc estimator with Leclerc-Laplacian Regularization are shown in Fig. 5.2(e-3) - Fig. 5.2(e-14) and Fig. 5.2(f-3) - Fig. 5.2(f-14) respectively.

From the result, the L2 estimator gives the best result for SRR estimating at low noise power because the AWGN distributional characteristic is a quadratic model that similar to L2 model. However, at high noise power, the Hampel, Andrew's Sine, Geman&McClure and Leclerc Norm estimator give the better result than L2 estimator since the L2 norm is very sensitive to outliers where the influence function increases linearly and without bound.

5.1.1.3 Poisson Noise

The original HR image is shown in Fig. 5.2(g-1) and one of corrupted LR images is shown in Fig. 5.2(g-2). The L2, estimator, Hampel estimator (with Hampel-Laplacian Regularization) and Andrew's Sine estimator (with Andrew's Sine-Laplacian Regularization) give the highest PSNR from experimental results.

The result of L1 estimator with Laplacian Regularization, L1 estimator with BTV Regularization, L2 estimator with Laplacian Regularization, L2 estimator with BTV Regularization, Hampel estimator with Laplacian Regularization, Hampel estimator with Hampel-Laplacian Regularization, Andrew's Sine estimator with Laplacian Regularization, Geman&McClure estimator with Laplacian Regularization, Geman&McClure estimator with Laplacian Regularization, Geman&McClure-Laplacian Regularization, Leclerc estimator with Laplacian Regularization and Leclerc estimator with Leclerc-Laplacian Regularization are shown in Fig. 5.2(g-3) - Fig. 5.2(g-14) respectively.

From the result, the Hampel, Andrew's Sine, Geman&McClure and Leclerc Norm estimator give the best result since the power of noise is slightly high and the distribution of noise is not a quadratic model (the L2 estimator can not estimate the nonquadratic model effectively).

5.1.1.4 Salt&Pepper Noise

This experiment is a 3 Salt&Pepper Noise cases at D=0.005, D=0.010 and D=0.015 respectively and the original HR images are shown in Fig. 5.2(h-1) – Fig. 5.2(j-1) respectively. The corrupted images at D=0.005, D=0.010 and D=0.015 are showed in Fig. 5.2(h-2), Fig. 5.2(i-2) and Fig. 5.2(j-2) respectively. The Hampel, Andrew's Sine, Geman&McClure and Leclerc Norm estimator results give dramatically higher PSNR than L1 estimator result (with Laplacian and BTV Regularization result) and L2 estimator result (with Laplacian and BTV Regularization result).

At D=0.005, D=0.010 and D=0.015, the result of L1 estimator with Laplacian Regularization, L1 estimator with BTV Regularization, L2 estimator with Laplacian Regularization, L2 estimator with BTV Regularization, Hampel estimator with Laplacian

Regularization, Hampel estimator with Hampel-Laplacian Regularization, Andrew's Sine estimator with Laplacian Regularization, Andrew's Sine estimator with Andrew's Sine-Laplacian Regularization, Geman&McClure estimator with Laplacian Regularization, Geman&McClure estimator with Geman&McClure-Laplacian Regularization, Leclerc estimator with Laplacian Regularization and Leclerc estimator with Leclerc-Laplacian Regularization are shown in Fig. 5.2(h-3) - Fig. 5.2(h-14), Fig. 5.2(i-3) - Fig. 5.2(i-14) and Fig. 5.2(j-3) - Fig. 5.2(j-14) respectively.

From the results, the Hampel, Andrew's Sine, Geman&McClure and Leclerc Norm estimator outperform the other estimators when the image is corrupted by Salt&Pepper Noise about 4-5 dB. The Hampel, Andrew's Sine, Geman&McClure and Leclerc Norm estimators give the better result for SRR estimating than L1 or L2 estimator because these robust estimators are designed to be robust and reject outliers. Their norms are more forgiving outliers; that is, the norm should increases less rapidly than L2.

5.1.1.5 Speckle Noise

The last experiment is a 3 Speckle Noise cases for 40th frame Susie sequence at V=0.01, V=0.02 and V=0.03 respectively. The original HR images are shown in Fig. 5.2(k-1) – Fig. 5.2(m-1) respectively. The corrupted images at V=0.01, V=0.02 and V=0.03 are shown in Fig. 5.2(k-2), Fig. 5.2(l-2) and Fig. 5.2(m-2) respectively.

At low noise power (V=0.01), the L2 estimator result (with Laplacian and BTV Regularization) give slightly higher PSNR than Hampel, Andrew's Sine, Geman&McClure and Leclerc Norm estimator results. However, L2, Hampel, Andrew's Sine, Geman&McClure and Leclerc Norm estimator result have higher PSNR than L1 estimator result (with Laplacian and BTV Regularization). The result of L1 estimator with Laplacian Regularization, L1 estimator with BTV Regularization, L2 estimator with Laplacian Regularization, Hampel estimator with BTV Regularization, Hampel estimator with Laplacian Regularization, Andrew's Sine estimator with Laplacian Regularization, Andrew's Sine-Laplacian Regularization, Geman&McClure estimator with Laplacian Regularization, Geman&McClure-Laplacian Regularization, Leclerc estimator with Laplacian Regularization and Leclerc estimator with Leclerc-Laplacian Regularization are shown in Fig. 5.2(k-3) - Fig. 5.2(k-14) respectively.

At high noise power (V=0.02 and V=0.03), the Hampel, Andrew's Sine, Geman&McClure and Leclerc Norm estimator result give the best performance than L2 estimator result (with Laplacian and BTV Regularization), L1 estimator result (with Laplacian and BTV Regularization). At V=0.02 and V=0.03, the result of L1 estimator with Laplacian Regularization, L1 estimator with BTV Regularization, L2 estimator with Laplacian Regularization, Hampel estimator with Laplacian Regularization, Hampel estimator with Hampel-Laplacian Regularization, Andrew's Sine estimator with Laplacian Regularization, Geman&McClure estimator with Laplacian Regularization, Geman&McClure estimator with Laplacian Regularization, Leclerc estimator with Laplacian Regularization and Leclerc estimator with Leclerc-Laplacian Regularization are shown in Fig. 5.2(l-3) - Fig. 5.2(l-14) and Fig. 5.2(m-3) - Fig. 5.2(m-14) respectively.

From the results, the Hampel, Andrew's Sine, Geman&McClure and Leclerc Norm estimator efficiently reconstruct the image that is corrupted by Speckle Noise at high noise power. It performs better than L1 and L2 estimator because Hampel, Andrew's Sine,

Geman&McClure and Leclerc Norm estimator is more robust against the high power outliers than L1 and L2 estimators.



Figure 5.2: The experimental result of SRR algorithm using the proposed robust estimation technique (Susie Sequence : The 40th Frame)



Figure 5.2: The experimental result of SRR algorithm using the proposed robust estimation technique (Susie Sequence : The 40th Frame) (Con.)



Figure 5.2: The experimental result of SRR algorithm using the proposed robust estimation technique (Susie Sequence : The 40th Frame) (Con.)

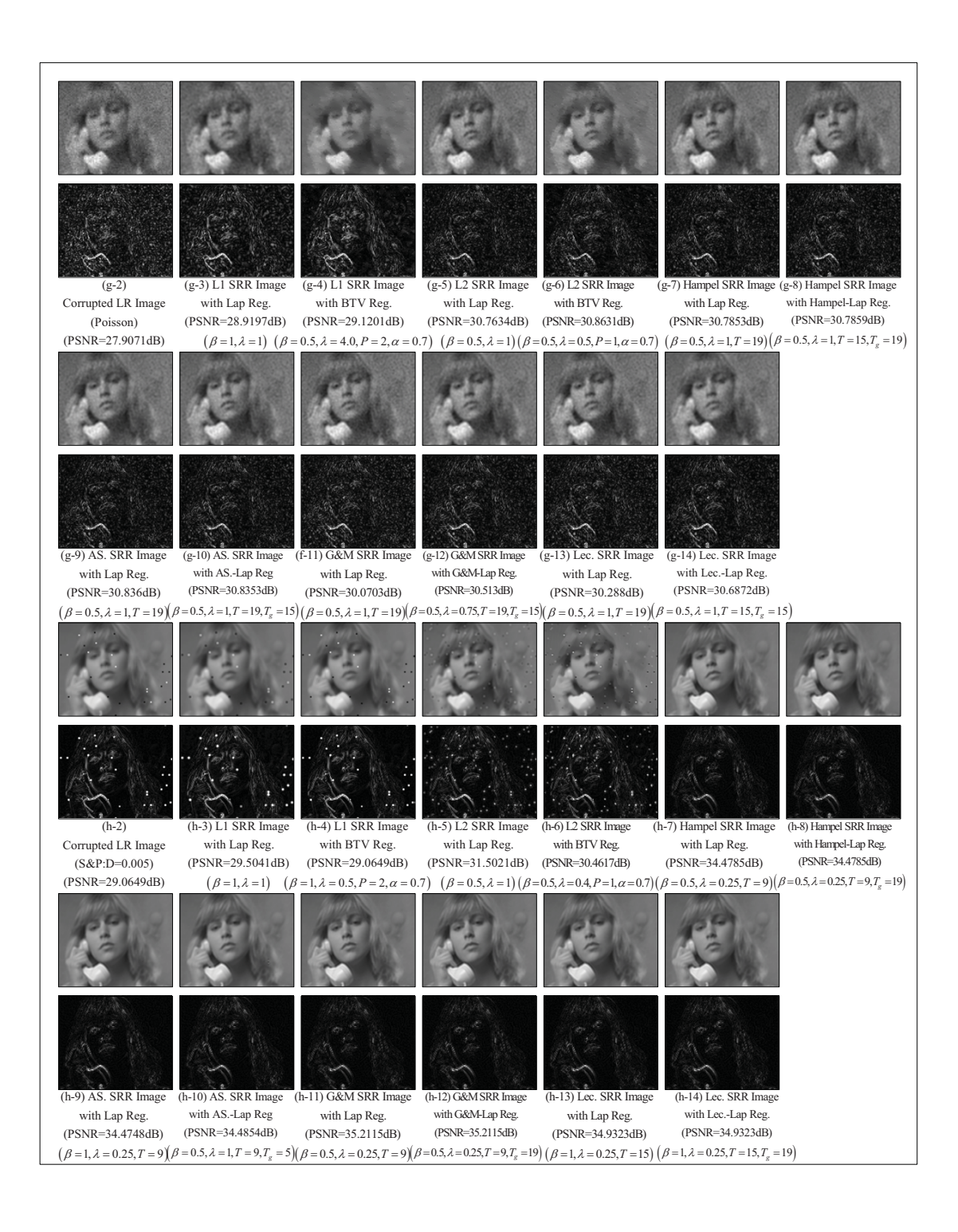


Figure 5.2: The experimental result of SRR algorithm using the proposed robust estimation technique (Susie Sequence : The 40th Frame) (Con.)

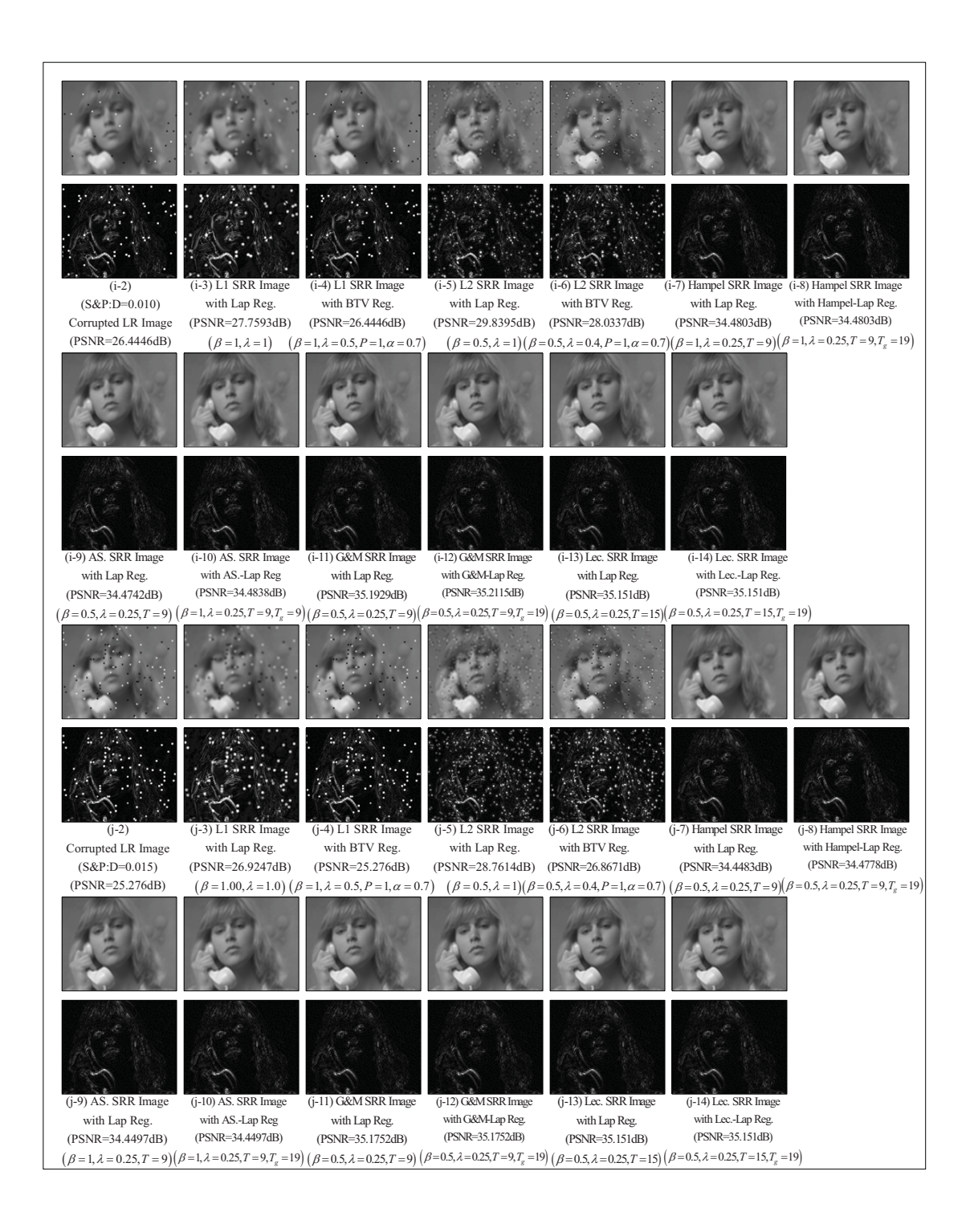


Figure 5.2: The experimental result of SRR algorithm using the proposed robust estimation technique (Susie Sequence : The 40th Frame) (Con.)



Figure 5.2: The experimental result of SRR algorithm using the proposed robust estimation technique (Susie Sequence : The 40th Frame) (Con.)

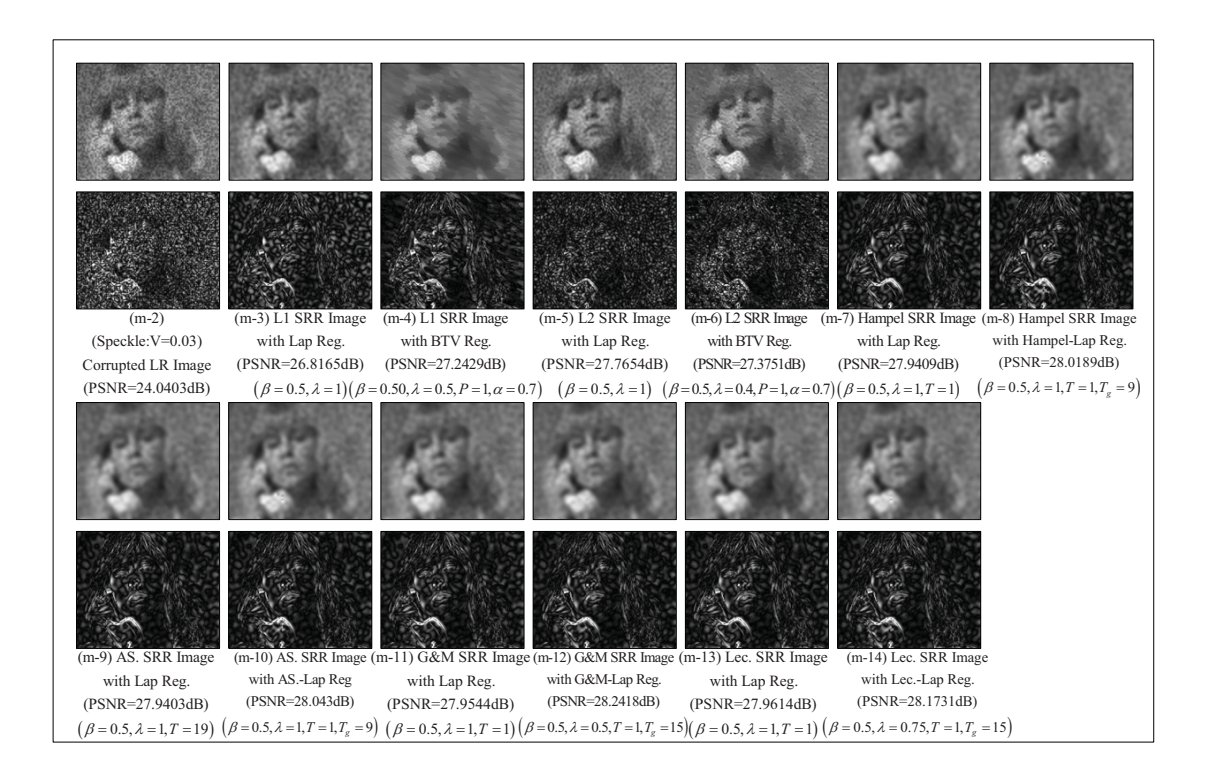


Figure 5.2: The experimental result of SRR algorithm using the proposed robust estimation technique (Susie Sequence : The 40th Frame) (Con.)

5.1.1.6 Experimental Conclusion on Susie Sequence (40th Frame)

From all experimental results of Susie Sequence (40th Frame) are shown in Fig. 5.2 respectively, all comparatively experimental results are concluded as follow:

- The SRR algorithm using Hampel, Andrew's Sine, Geman&McClure and Leclerc Norm norm with the proposed registration gives the highest PSRN especially for high power noise.
- For Salt&Pepper Noise cases, the Hampel, Andrew's Sine, Geman&McClure and Leclerc Norm estimator give the far better reconstruction than L1 and L2 estimator because these robust estimators are designed to be robust and reject outliers. The norms are more forgiving on outliers; that is, they should increase less rapidly than L2.
- The SRR algorithm using L1 norm with the proposed registration gives the lowest PSRN because the L1 norm is excessively robust against the outliers.